THE JOURNAL OF PHYSICAL CHEMISTRY B

Subscriber access provided by Universitätsbibliothek Bern

B: Biomaterials and Membranes

Interactions of Cationic Diruthenium Trithiolato Complexes With Phospholipid Membranes Studied by NMR Spectroscopy

Hedvika Primasová, Martina Vermathen, and Julien Furrer

J. Phys. Chem. B, **Just Accepted Manuscript** • DOI: 10.1021/acs.jpcb.0c05133 • Publication Date (Web): 15 Sep 2020

Interactions of Cationic Diruthenium Trithiolato Complexes with Phospholipid Membranes Studied by NMR Spectroscopy

*Hedvika Primasová *, Martina Vermathen * and Julien Furrer **

Department of Chemistry and Biochemistry, University of Bern, Freiestrasse 3, CH-3012 Bern, Switzerland

KEYWORDS ruthenium complex, hydrophobic cation, interaction, membrane model, liposome, micelle, phospholipid, nuclear magnetic resonance

ABSTRACT. To apprehend the possible mechanisms involved in the cellular uptake and the membrane interactions of cytotoxic dinuclear *p*-cymene trithiolato ruthenium(II) complexes, the interactions of the complexes $[(\eta^6\text{-}p\text{-}MeC_6H_4Pr^i)_2Ru_2(R^1)_2(R^2)]^+$ ($R^1 = R^2 = SC_6H_4\text{-}m\text{-}Pr^i$:**1**; $R^1 = SC_6H_4\text{-}p\text{-}OMe$, $R^2 = SC_6H_4\text{-}p\text{-}OH$:**2**; $R^1 = SCH_2C_6H_4\text{-}p\text{-}OMe$, $R^2 = SC_6H_4\text{-}p\text{-}OH$:**3**) with 1,2-dioleoyl-*sn*-glycero-3-phosphocholine (DOPC) vesicles and

1,2-dihexanoyl-*sn*-glycero-3-phosphocholine (DHPC) micelles were studied using nuclear magnetic resonance (NMR) spectroscopy. ^{1}H, NOE, DOSY, and T_1 and T_2 relaxation data provided information on interactions between the complexes and the model membranes and on the submolecular localization of the complexes at the membrane interface. The results suggest that (a) interaction takes place without new covalent adduct formation, (b) the cationic diruthenium complexes interact with DOPC head groups most likely involving electrostatic interactions while remaining structurally unchanged, (c) the changes indicating interactions are more pronounced for the most lipophilic complex **1**, (d) the diruthenium complexes remain at the exterior vesicle surface and unlikely insert between the phospholipid chains. The complexes also interact with micellar/free DHPC and seem to induce micellization or aggregation in sub-CMC solutions. Our study suggests a high affinity of the Ru complexes for the membrane surface that likely plays a key role in cellular uptake and possibly also in redistribution to mitochondria.

INTRODUCTION In recent years, our group has focused on the development of cationic dinuclear thiolato-bridged arene Ruthenium(II) complexes (in the following named *diruthenium complexes*) as anti-cancer and antiparasite agents.[1–5] The trithiolato diruthenium complexes of the general formula $[(\eta^6\text{-arene})_2Ru_2(\mu\text{-}SR)_3]^+$ and $[(\eta^6\text{-arene})_2Ru_2(\mu\text{-}SR_1)_2(\mu\text{-}SR_2)]^+$ are highly cytotoxic against ovarian cancer cell lines A2780 and their cis-Pt resistant analogs A2780cisR.[1] The most active derivative $[(\eta^6\text{-}p\text{-}MeC_6H_4Pr^i)_2Ru_2(\mu_2\text{-}S\text{-}p\text{-}C_6H_4Bu^t)_3]Cl$, termed diruthenium-1 or DiRu-1, has an IC_{50} value of 30 nM in both cell lines. It has also shown *in vivo* activity as it significantly prolonged the survival of tumor-bearing mice.[6] DiRu-1 is among the most cytotoxic Ru complexes reported to date.[1]

The trithiolato diruthenium complexes are stable under physiological conditions. While the exact mechanism of action is not completely clear yet, it has been shown that they are able to catalyze glutathione (GSH) and cysteine (Cys) oxidation and to induce reactive oxygen species (ROS) burst and DNA lesion formation, which can all lead to apoptosis and cell cycle arrest in treated cancer cells.[6–9] Recently, it has been shown using ICP-MS that treatment of cancer cells with other very similar diruthenium complexes results in a

specific accumulation of Ru in mitochondria.[5] Likewise, Ru was found in mitochondria of *T. gondii* treated with other again comparable diruthenium complexes.[10] Additionally, structural changes in mitochondria were observed by TEM in *N. caninum* treated with these complexes.[5] However, the exact location of Ru within mitochondria is not known yet.[5,10]

In order to enter cells and subsequently cell-organelles, the drug needs to cross the plasma membrane, which takes place mostly via passive diffusion, with the help of transporters, or via endocytosis. Whether the drug will pass via passive diffusion depends on factors such as lipophilicity, ability to form H bonds, charge and size of the drug, pH of the system, and membrane potential.[11,12] Hydrophilic molecules usually are not able to cross the plasma membrane without the help of membrane transporters, and charged molecules encounter the problem of crossing the hydrophobic core of a bilayer.[13] Lipophilic cations, on the other hand, are known to be able to passively diffuse through membranes.[14,15]

If an organometallic compound does not act as a prodrug, like CO-releasing organometallic compounds *in vivo*,[16] one of the most important prerequisites for

preventing side effects and general toxicity is that the compound enters cells virtually intact, which requires that no or only weak interactions, such as hydrogen bonds, between the compound and cell membranes exist. The chemical nature of the surrounding ligands strongly influences the propensity of the metal to be oxidized or reduced and triggers the potential interactions with the cell membranes. The factors influencing the toxicity and efficacy of diruthenium complexes are lipophilicity and Hammett coefficient of the aromatic thiol.[1,17] For instance, the complexes having Hammett constants in the range of -0.2 to 0 and partition coefficients between 3.0 and 4.0 are those showing the lowest IC_{50} values.[17]

As biological membranes are structurally and composition-wise complex, simplified artificial model membranes are often studied. There are three model systems commonly used – planar lipid monolayers, supported bilayers and liposomes.[18,19] Liposomes are spherical phospholipid vesicles containing an aqueous compartment. This model is suitable for studies of drug membrane permeability.[20] Additionally to the already mentioned models, micelles can be used as a simple model of lipid membranes when investigating interactions.[21] Compared to liposomes, micelles are very dynamic species

coexisting with the free form of their components in solution.[22] Micelles are easy to prepare, and nuclear magnetic resonance (NMR) spectra of micellar solutions show narrower linewidths as compared to phospholipid liposome suspensions. Although micelles have some limitations due to their monolayered structure, their enhanced dynamics may offer important complementary information on potential sites of interactions between the micellar amphiphiles and the drug molecules.

NMR spectroscopy is a technique that offers numerous possibilities to study interactions between lipid model membranes and drugs. It allows obtaining information on diffusion rates and therefrom particle sizes, changes in molecular surroundings, proximity between two species, and kinetics like relaxation or exchange processes. Using NMR spectroscopy, the location of a guest molecule at the vesicle or micelle interface, aggregation, encapsulation and other aspects of drug-membrane interactions can be studied.[23–32]

This study is aiming to provide an insight into the interactions of diruthenium complexes with cell membranes. For this purpose, three representative complexes $[(\eta^6\text{-}p\text{-}MeC_6H_4Pr^i)_2Ru_2(R_1)_2(R_2)]^+$ with different degrees of lipophilicity and in vitro cytotoxicity

($R_{1,2}$ = SC_6H_4-*o*-^{i}Pr: **1**; R_1 = SC_6H_4-*p*-OMe; R_2 = SC_6H_4-*p*-OH : **2**; R_1 = $SCH_2C_6H_4$-OMe; R_2 = SC_6H_4-*p*-OH : **3**) were selected (Figure 1) and their interactions towards the membrane models 2-dioleoyl-*sn*-glycero-3-phosphocholine (DOPC) vesicles and 1,2-dihexanoyl-*sn*-glycero-3-phosphocholine (DHPC) micelles were studied with NMR spectroscopy as main tool. Even though, DHPC has rather detergent than lipid-like properties, it will be referred to as (short chain) phospholipid here to underline its close chemical relationship as a phosphatidylcholine with DOPC.

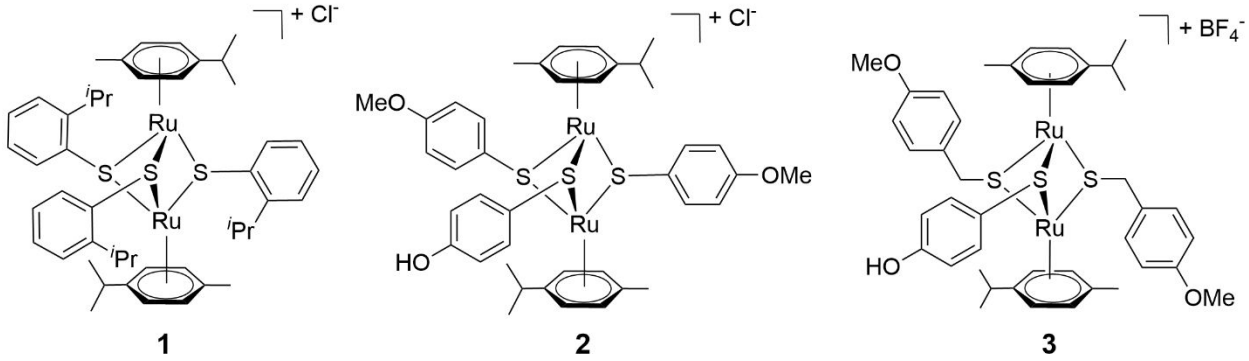

Figure 1. Structures of the three diruthenium complexes (**1**-**3**) investigated in this work.

EXPERIMENTAL

Materials: The diruthenium complexes **1-3** were synthesized according to published methods.[3,33,34] All chemicals were used as received. 1,2-dioleoyl-*sn*-glycero-3-

phosphocholine (DOPC) and 1,2-dihexanoyl-*sn*-glycero-3-phosphocholine (DHPC) were obtained from Avanti Polar Lipids Inc. KH_2PO_4 and Na_2HPO_4 were purchased from Sigma Aldrich. Deuterated solvents were obtained from Cambridge Isotope Laboratories, Inc, $PrCl_3$ from Aldrich Chem. Co.

Phosphate buffered saline (PBS) solution was prepared from aliquots of 50 mM KH_2PO_4 and 50 mM Na_2HPO_4 solutions containing 0.9% NaCl in D_2O to reach a pD corresponding to measured pH of 7.0. Unless otherwise specified, the interaction experiments were performed in deuterated PBS/dDMSO 4:1 ($pD^{mixture}$ corresponding to measured pH of 7.7) to allow dissolution of the sparingly soluble diruthenium complexes **1-3**.

Preparation of liposomes: DOPC vesicles were freshly prepared before every new set of experiments. DOPC was dissolved in chloroform in a glass vial, and the solvent was subsequently evaporated upon an argon stream to leave a uniform lipid film on the walls. The residual solvent was removed in vacuo. The resulting homogeneous film was hydrated with PBS by vortexing to obtain a 12.5 mM DOPC suspension. The suspension was subsequently sonicated for 30 min at room temperature in the center of an ultrasonic

bath. When the DOPC vesicles were investigated alone, dDMSO was added to the prepared vesicles to obtain a final DOPC concentration of 10 mM.

Preparation of micelles: Critical micelle concentration (CMC) of DHPC in PBS/dDMSO 4:1 and at 310 K was determined using 2D ^{1}H Diffusion Ordered SpectroscopY (DOSY) NMR.[35,36] DOSY spectra of DHPC solutions of incremented concentrations were recorded, and the resulting diffusion coefficients obtained from processed DOSY pseudo-2D spectra were plotted against the log of the concentration. The CMC (25 mM, Figures S1-3) was estimated to lie at the intersection of two linear regions.[35] Subsequently, 28 mM DHPC solution in PBS/dDMSO 4:1 was prepared.

Mixtures of diruthenium complexes with phospholipids: The diruthenium complexes **1**, **2,** and **3** were dissolved in dDMSO to give 5 mM stock solutions. Note that the complexes are stable in dDMSO over a long period.[1,9] In order to investigate the interactions with lipid membrane models, 20 µL of each complex solution in dDMSO was gently mixed with 80 µL of a suspension of lipid vesicles or micelles in deuterated PBS, respectively. Mixtures of 1 mM complex and 10 mM DOPC vesicles or 28 mM DHPC, respectively, resulted. When the diruthenium complexes were investigated alone, pure PBS was added

to reach 1 mM solutions. For NOE NMR experiments (see below), 800 µL of the sample were prepared.

An alternative preparation method involving hydration of the film formed by the complex and the lipid (co-dissolved in organic solvent) after solvent removal in PBS and subsequent addition of a corresponding amount of dDMSO was used to test the effect of co-dissolution in comparison to the addition of **1-3** to preformed vesicles.[37] For this, DOPC and each diruthenium complex were dissolved in chloroform, which subsequently was evaporated and the flask with the resulting film dried in vacuo as described above. PBS was added to the film, the flask vortexed followed by 30 min sonication at room temperature to give a suspension containing the diruthenium complex and DOPC vesicles. After sonication, dDMSO was added. The resulting concentrations of the diruthenium complex and DOPC in PBS/dDMSO 4:1 were 1 mM and 10 mM, respectively.

NMR spectroscopy: ^{1}H- and ^{31}P-spectra, T_1 and T_2 relaxation measurements, and DOSY spectra were recorded on a Bruker Avance II NMR spectrometer operating at a nominal ^{1}H frequency of 500.13 Hz. The spectrometer is equipped with a triple resonance

(^{1}H, ^{13}C, ^{31}P) 1.7 mm microprobehead with additional z-gradients. 1D NOE and spectra needed for the characterization of the complexes (^{13}C, COSY, HSQC, HMBC) were recorded on a Bruker Avance III spectrometer operating at 400.13 MHz equipped with a 5 mm ATM BBFO SmartProbe®. All NMR spectra were recorded at a regulated temperature of 310 K. Processing and analysis were performed using TopSpin 3.5-6 (Bruker). For DOSY, T_1, and T_2 measurements, Dynamics Center 2.4.2 (Bruker) was used for data fitting.

1D ^{1}H and ^{31}P NMR spectroscopy: 1D ^{1}H NMR spectra were recorded using the *zgpr30* (Bruker) pulse sequence for presaturation of the residual water resonance. 1D ^{31}P NMR spectra were obtained using the *zgpg* sequence (Bruker) with broadband ^{1}H decoupling. The diruthenium complexes were mixed with phospholipid vesicles or micelles just before measurements. For the ^{1}H NMR spectra, the relaxation delay was set to 1 s and the spectral width to 7352.9 Hz. The irradiation frequency was set individually to the center of the residual water peak (at approximately 4.7 ppm). Unless otherwise stated, the acquisition time was 1.11 s, 128-256 scans were recorded, and processing involved line broadening of 2 Hz, Fourier transformation, phase correction, and automatic baseline

correction. ^{31}P spectra were recorded with 32 scans, a spectral width of 40760.87 Hz, 32768 data points, an acquisition time of 0.402 s, and a relaxation delay of 2 s unless otherwise specified.

NOE spectroscopy: 1D NOE spectra were recorded using a modified pulse program *1dnoesy* derived[38] from the standard *selnogp* pulse program (Bruker) with the relaxation delay set to 1 s, the acquisition time to 511 ms and the spectral width to 8012.8 Hz. 2048 scans were recorded. The mixing time was set to 100 ms to minimize the effects of spin diffusion. The N-methyl and the $(CH_2)_n$ resonances of the phospholipid chain and one resonance of the aromatic thiol of the diruthenium complex were irradiated in separate experiments to obtain information on the possible location of the complex within the membrane. The frequencies irradiated are indicated in the relevant spectra (Figures 2 and S4-6).

Diffusion ordered spectroscopy: 2D ^{1}H DOSY experiments were performed using a stimulated echo bipolar gradient pulse sequence *ledbpcpgp2scpr* (Bruker) with longitudinal Eddy current delay, 2 spoil gradients and presaturation of the water resonance.[39] The diffusion time was set to 80 ms, and the relaxation delay to 1 s. The gradient strength was linearly varied (2-98%) to reach optimal signal attenuation. At

each gradient strength, 128 scans were recorded in 0.68 s acquisition time. The gradient strength of our probehead is 5.35 G/cmA. Typically, the gradient pulse length was set to 2-4.5 ms, and the diffusion list contained 24 values in the range of 2-98% of the maximum gradient strength. All single spectra from the DOSY experiments (series of 1D spectra) were processed with exponential multiplication applying a line broadening factor of 3 Hz prior to fitting in Dynamics Center. The examples of fitting plots for DOPC and DHPC can be found in SI (Figures S7-8), the program was used on selected peak regions excluding HDO and DMSO. The diffusion coefficient D was obtained from fitting using the Stejskal-Tanner equation (1)[40] where I is the signal intensity, I_0 the respective signal intensity at zero gradient, γ the gyromagnetic ratio of ^{1}H, g the gradient strength, δ the gradient length and Δ the delay between dephasing and rephasing gradients.

$$I = I_0 \exp\left[\gamma^2 g^2 \delta^2 \left(\Delta - \frac{\delta}{3}\right) D\right] \qquad (1)$$

The hydrodynamic radius of DHPC micelles was estimated from DOSY NMR results according to the Stokes-Einstein equation (2) where D is the diffusion constant, k the Boltzmann constant,

$$D = \frac{kT}{6\pi\eta R} \qquad (2)$$

T the temperature, η the viscosity of the medium, and *R* the radius of the particle under the assumption that DHPC micelles have an approximately spherical shape. Obstruction effects were not included in the calculation. The viscosity of the mixtures was determined experimentally using a rotary rheometer (see “Dynamic light scattering” below).

Relaxation time measurements: The inversion recovery experiment employing the standard *t1irprf1* (Bruker) sequence with presaturation of the water resonance was used to determine the longitudinal relaxation time T_1. Depending on the sample, (diruthenium complexes, phospholipids alone, or a mixture), the relaxation delay was set to 4-10 s with variable interpulse delay lists containing 16-18 increments in the range of 0.001-9 s, with 32-128 scans for each delay value.

Transverse relaxation times T_2 were measured using the Carr-Purcell-Meiboom-Gill (CPMG) sequence[41,42] *cpmgpr* (Bruker) with presaturation of the water resonance. The relaxation delay was set to 10 s. The spin-echo delay was incremented with 19 values in the range of 8 – 3000 ms suitable for both the ruthenium complexes and the lipids. Depending on the sample, the number of scans was set to 32 or 64 for each increment.

Lanthanide shift experiments: The lanthanide shift experiments were performed with complex **1**, the most soluble among the three diruthenium complexes, by adding praseodymium (III) chloride $PrCl_3$ (0.05 mM; 0.1 mM; 1 mM; 5 mM; 10 mM) in a mixture D_2O/dDMSO (1:4), respectively, to induce broadening and shift of lipid resonances from the outer layer to distinguish the vesicle exterior surface from interior.[43] D_2O was used instead of PBS to improve solubility. Using the optimal concentration (with respect to induced shift and resulting lineshapes) of $PrCl_3$ at 1 mM, ^1H and ^{31}P spectra of DOPC vesicles in D_2O/dDMSO in the presence of **1** (1 mM) and the lanthanide shift reagent were recorded. ^{31}P spectra were recorded using the following acquisition parameters: 6144 scans, spectral width of 40760.87 Hz, 8192 data points, acquisition time of 0.10 s, and relaxation delay of 1 s. ^1H spectra were recorded with 256 scans, spectral width of 7352.94 Hz, 16384 data points, acquisition time of 1.11 s, and relaxation delay of 1 s.

Dynamic light scattering: Dynamic light scattering (DLS) was used to estimate the hydrodynamic radius in the case of DOPC vesicles. DLS measurements were performed with the Anton Paar Litesizer 500, using acrylic cuvettes (1 cm path length) and a 660 nm laser in backscattering mode with 60 runs (time per run 10 s). Data were processed using

the Kalliope 2.8.3 software. For both methods, DOSY NMR and DLS, the viscosity of solutions and suspensions, respectively, was determined using the rotary rheometer Anton Paar MCR 92. NMR, DLS, and viscosity measurements were all performed at a regulated temperature of 310 K.

Mass spectrometry: Electron spray ionization mass spectra of mixtures were recorded in positive mode using an LTQ Orbitrap XL spectrometer with nano ESI (Thermo).

RESULTS AND DISCUSSION

Characterization of the diruthenium complexes: In Table 1, the calculated log *P* values for the different thiol ligands of complexes **1-3** are given, indicating their lipophilicity. **1** is the most lipophilic of the three complexes, and is, *in vitro*, one order more cytotoxic in terms of IC_{50} compared to **3.**[3,33] This correlation between lipophilicity and cytotoxicity was to some extent observed and reported for other complexes of this family against parasites[5,10] and against cancer cells: the sum of the calculated log *P* values for the thiol

ligands of the most cytotoxic complexes range between 9 and 13.[44] The lipophilicity can be expected to play a role in interactions with biological membranes.[11,45]

Table 1. log *P* values of the different thiol ligands (HS-R), the sum of the individual values, and cytotoxicities of the complexes in terms of IC_{50} values against A2780 cell line and its cisplatin-resistant variant (cisR).[3,33] The log *P* values have been calculated using ChemDraw 19.0.

	R_1	log *P*	R_2	log *P*	Σ	IC_{50} [μM]
1	SC_6H_4-*o*-^{i}Pr	3.96	SC_6H_4-*o*-^{i}Pr	3.96	11.88	**A2780:** 0.030 ± 0.001 **A2780cisR:** 0.031 ± 0.001
2	SC_6H_4-*p*-OMe	2.54	SC_6H_4-*p*-OH	1.87	6.95	-
3	$SCH_2C_6H_4$-*p*-OMe	2.33	SC_6H_4-*p*-OH	1.87	6.53	**A2780:** 0.32 ± 0.08 **A2780cisR:** 0.109 ± 0.03

The use of DMSO as a co-solvent was unavoidable for the three complexes as their solubility in pure 50 mM PBS is too low for the envisaged NMR studies. Out of the three complexes, **1** was the easiest to dissolve, followed by **2**. This ease of dissolution for **1** was unexpected, since it is by far the most lipophilic among the three complexes. The different counterion present with **1** and **2** on the one hand (Cl^-) and with **3** (BF_4^-), on the

other hand, may have an influence on their solubility in mixtures PBS/DMSO, but this was not further investigated.

Characterization of the model membrane systems: Above CMC, micelles, and free phospholipid coexist, and their ratio depends on the total concentration of the phospholipid. From the diffusion coefficient D of free DHPC in solution below CMC and the average D at a concentration above CMC used for the interaction experiments (28 mM), D of micelles was calculated to be $3.16 \cdot 10^{-11}$ m^2/s using relation (3)[46,47]. Assuming that only micellar and free phospholipid species are present, the following relation (3) is valid where D^{tot} is the diffusion coefficient for the 28 mM DHPC solution, D^{free} for the solution of 10 mM DHPC containing only free species, D^m is the diffusion coefficient of the micelles to be determined, and c^{tot} and c^{free}, respectively, are the corresponding concentrations.

$$D^{tot} = D^m \frac{(c^{tot} - c^{free})}{c^{tot}} + D^{free} \frac{c^{free}}{c^{tot}} \quad (3)$$

The calculated hydrodynamic radius of DHPC micelle is then 4.66 nm. The value is higher compared to the values commonly reported for DHPC micelles prepared in water or

aqueous buffers.[46,48,49] It has been reported that solvents can have an influence on CMC, micelle size or size of vesicles.[50–52] In our case, the medium contains 20% DMSO and D_2O instead of H_2O, which both may contribute to the size deviation.

DOPC liposomes were characterized using DLS. For a 10 mM suspension of DOPC vesicles in PBS/DMSO (D_2O), an average hydrodynamic radius of 83 nm was found with a polydispersity index (PDI) of 27.5% from number weighted distributions (Figure S9).

Interaction studies:

1D NMR: For the interaction studies, 1D ^{1}H NMR spectra of the pure components were first recorded, and subsequently 1D ^{1}H NMR spectra of the mixtures. Whenever necessary, 2D NMR spectra were acquired for completing/supporting the attribution of the proton resonances.

Single components: The chemical shifts of the different protons of the individual components (diruthenium complexes **1-3**, DHPC and DOPC) were in agreement with literature data, the slight differences being due to the different solvents used (Figures S10-11 and Tables S1-3).[3,33,53,54]

Mixtures: (i) Diruthenium complexes: Resonance broadening and small shift changes were observed in the regions containing the protons of the thiol ligand and *p*-cymene for all three diruthenium complexes upon addition of DOPC liposomes, suggesting the existence of weak non-covalent interactions (Figures S12-14 and Tables S1-3). If covalent bonds had been formed between **1-3** and phospholipid, more pronounced changes in chemical shift would have been expected. The absence of covalent bonds between **1-3** and DOPC, as well as the integrity of the complexes, was additionally confirmed by ESI-MS (Figures S15-17).

The linewidth of NMR resonances is proportional to the transverse relaxation rate $R_2 = 1/T_2$, which itself is proportional to the molecular mass or inversely proportional to the dynamic – given by the correlation time τ_c - of the molecule investigated. Thus, when a diruthenium complex interacts with the large DOPC vesicles, it acquires the slow dynamic of the latter, which in turn results in line broadening.

Mixed with DHPC (28 mM) micellar solution, **1-3** showed similar slight shift changes of several proton resonances (Figures S18-20 and Tables S1-3), but unlike what was observed with DOPC, no or a very small line broadening of the resonances of **1-3**

resulted, which is in line with the lower molecular mass of DHPC micelles compared to DOPC vesicles. Indeed, when a diruthenium complex interacts with the small DHPC micelles, the overall mass of the system (DHPC:complex) is not drastically changed, which in turn does not significantly affect the broadening of the resonances.

Furthermore, it was noticed that DOPC (and to a smaller extent also DHPC) helped the dissolution of the otherwise sparingly soluble **3**.

(ii) DOPC: No changes in the chemical shift or linewidths were observed for the DOPC signals in the presence of **1-3**, as shown for the presence of complex **1** in Figure S12 b and c.

(iii) DHPC: No substantial changes in the shift or linewidths were observed in the presence of **1-3**. Like DOPC, the resonances of DHPC were not affected upon the addition of the three diruthenium complexes, which can also be ascribed to the high molar ratio DHPC:complex (28:1).

^{31}P NMR: No changes were observed in the ^{31}P NMR spectra when **1-3** were added to DHPC micelles (Figure S21). In the case of DOPC, the ^{31}P phosphocholine resonance overlapped with the intense phosphate resonance of the buffer and was therefore hard to

evaluate. However, in pure D_2O, the phosphocholine resonance of DOPC vesicles – like the one of DHPC micelles - did not exhibit changes in the presence of the diruthenium complex **1,** either (see "*Lanthanide shift experiments*").

NOE: NOE experiments are long known to afford 1D difference spectra or 2D chemical shift correlation maps in which through-space connectivities can be traced out.[55,56] We therefore used NOE experiments to obtain information on the location of the complexes at the interface of the phospholipid vesicles or micelles. In our study, selective 1D NOE experiments were applied to allow for satisfactory S/N given the limited solubility of **1-3**. Upon addition of **1,** when irradiating the N-methyl protons of DOPC at 3.33 ppm, apart from intramolecular NOEs, and NOE at 1.6 ppm, which belongs to the methyl group of *p*-cymene was observed (proton H in Figure 2b). As the same negative NOE was observed upon the addition of **2** (Figure S4), which does not possess an isopropyl group on the thiol ligand, we can safely conclude that the observed NOE in the case of **1** indeed belongs to the methyl group of *p*-cymene. Irradiation of the DOPC methylene resonance at 1.37 ppm (Figure 2a) and of the diruthenium-complex aromatic proton resonances at 7.49 ppm (Figure 2c) did not give rise to intermolecular NOEs. Therefore, the only

intermolecular NOE observed is a hint that the diruthenium complex is likely to be located on the surface of the vesicle exterior or interior and not in between the layers. No NOE data are available for **3**, as this complex tends to precipitate over time during longer measurements.

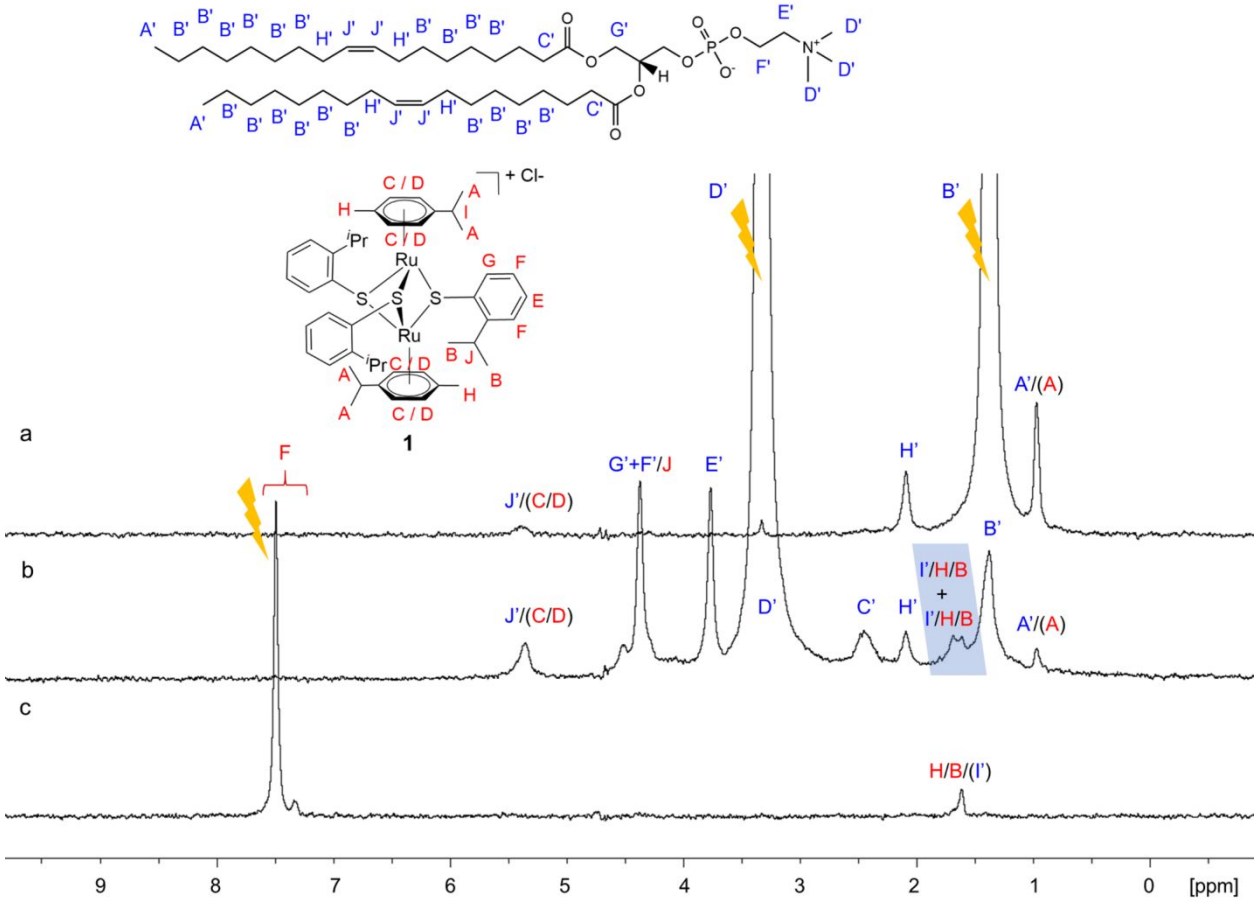

Figure 2. Superimposed 1D NOE NMR spectra of **1** (1 mM) and DOPC (10 mM) vesicles in PBS/DMSO. Irradiated (a): 1.367 ppm; (b): 3.328 ppm; (c): 7.494 ppm. Mixing time 100

ms, relaxation delay 1s, 2048 scans, 8192 TD data points, acquisition time 511 ms, spectral width 8012.8 Hz.

Upon addition of DHPC, no NOEs were observed between the diruthenium complexes and the phospholipid chain and headgroup – only intramolecular NOEs were visible (Figures S5 and S6).

Diffusion spectroscopy: When interacting with DOPC, the diffusion rate of the diruthenium complexes should approach or even reach the diffusion rate of the vesicles if we assume that all complexes interact with the vesicles. The DOSY spectra indeed showed that when the diruthenium complexes **1** and **3** interact with DOPC vesicles, their diffusion coefficient $D^{Ru\ complex}$ dropped to about the diffusion coefficient D^{DOPC} of the vesicles (Figures 3 and S22). $D^{Ru\ complex}$ also decreased, but to a smaller extent, in the case of **2,** which (a) is less soluble as compared to **1** and (b) exhibits a solubility that is not significantly improved in the presence of DOPC compared to **3**. The fact that no significant decrease of D^{DOPC} was observed in the presence of **1**-**3** is not surprising since

DOPC vesicles are much larger than **1-3**, and their whole mass will only slightly change upon interaction with the complexes **1-3.**

In the codissolution experiment, $D^{Ru\ complex}$ of **1** approached but did not reach D^{DOPC} (Figure 4a). This means that a fraction of the complex interacted with the vesicle while another fraction remained in solution. D^{DOPC}, on the other hand, seems to slightly decrease in the presence of **1**. No changes were observed in the codissolution experiment for **2** (Figure S23) as compared to the previous method (Fig. 3b). In the case of **3**, codissolution with DOPC prior to vesicle formation led to a better solubility of the complex. D^{DOPC} in the presence of **3** slightly decreased, as observed in the case of **1**. The diffusion coefficient of **3** decreased practically to the one of DOPC vesicles (Figure 4b). It is conceivable that the slight decrease of D^{DOPC} in the presence of **1** and **3**, occurs due to the presence of a higher amount of diruthenium complexes **1** and **3** associated with the vesicles, which is enabled by codissolution. No changes (nor in the chemical shift neither in the line broadening) were observed in the 1D ^{1}H NMR spectra of **1-3** upon codissolution with DOPC (Figure S24).

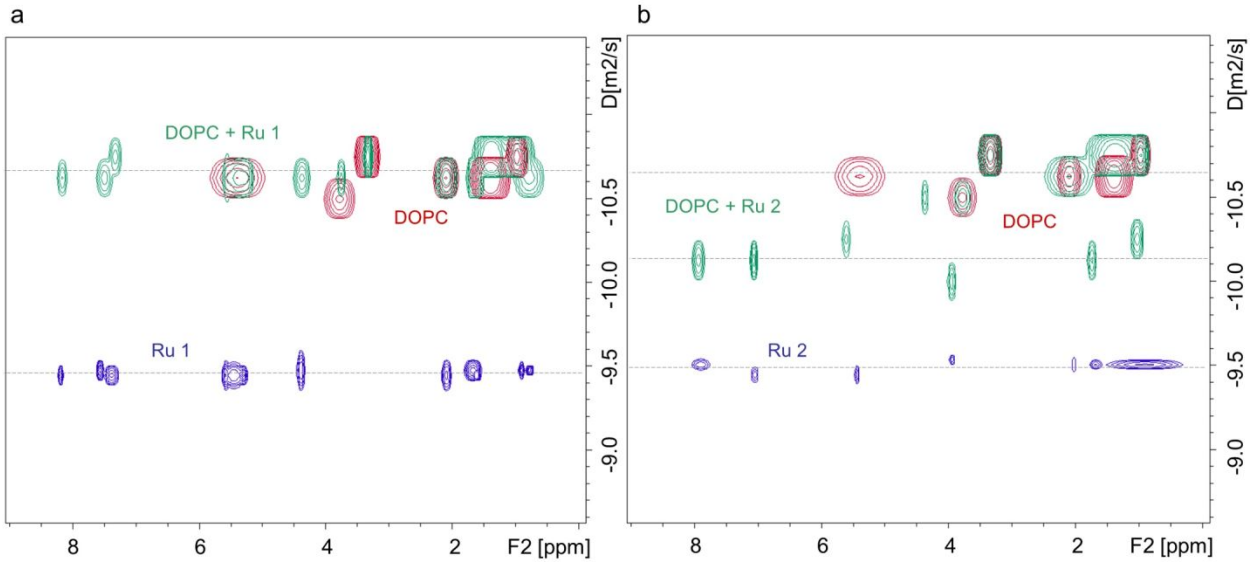

Figure 3. Overlay of DOSY spectra of (a): **1** (1 mM; blue), DOPC (10 mM; red) or mixture of both (green), respectively, dissolved in PBS (50 mM) / DMSO 4:1; (b): **2** (1 mM; blue), DOPC (10 mM; red) or mixture of both (green), respectively, dissolved in PBS (50 mM) / DMSO 4:1.

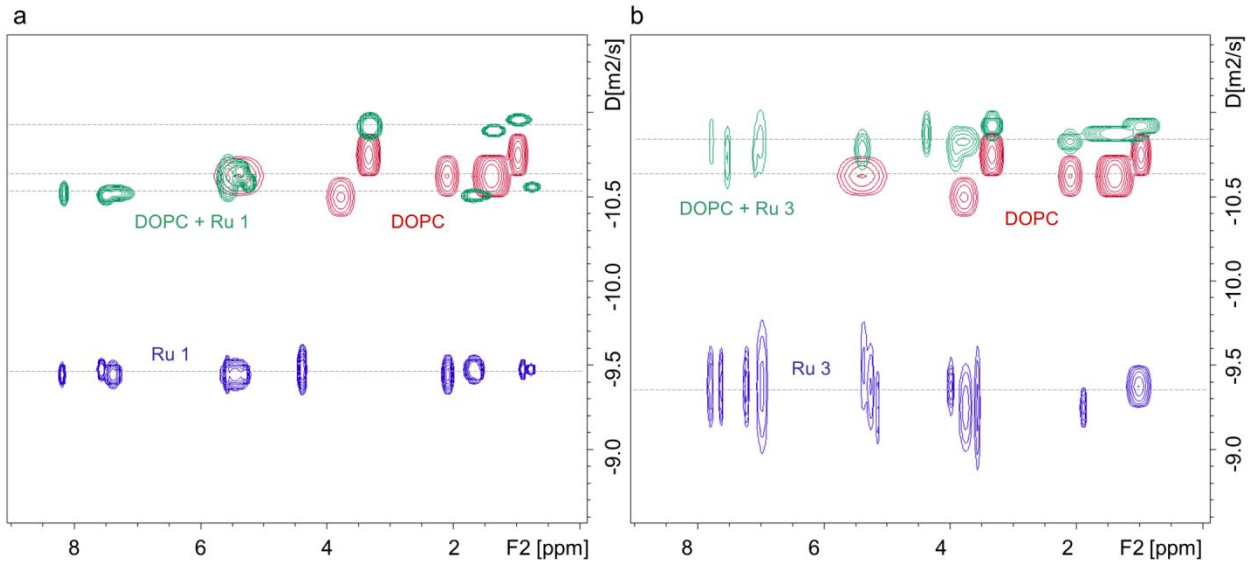

Figure 4. Overlay of DOSY spectra of (a): **1** (1 mM; blue), DOPC (10 mM; red) and **1** codissolved with DOPC upon vesicle formation in PBS (50 mM) / DMSO 4:1 (green); (b): **3** (1 mM; blue), DOPC (10 mM; red) and **3** codissolved with DOPC upon vesicle formation in PBS (50 mM) / DMSO 4:1 (green).

The diffusion coefficient $D^{Ru\ complex}$ of **1** and **2** decreased significantly (Figure 5) upon the addition of DHPC, while D^{DHPC} remained almost unchanged. In contrast to **1** and **2**, $D^{Ru\ complex}$ of **3** remained unchanged (Figure S25). As already mentioned at the beginning of this section, it needs to be considered that DHPC is present in two forms (micellar and free) in solution. Diffusion coefficients observed for DHPC are a weighted average of free and micellar species, free species being the major contributor. Here we should mention that due to limited solubility of **1-3** it was not possible to use DHPC at a concentration where most of the phospholipid would be present as micelles. At this concentration, the NMR resonances of the diruthenium complexes **1-3** would be barely visible. As the sparingly soluble complexes **1** and **2** interact with or become a part of micelles, their diffusion coefficients become smaller than the average diffusion coefficient of DHPC.

Accordingly, these $D^{Ru\ complex}$ values obtained for the diruthenium-complexes represent **1** and **2** associated with micelles. The D^{DHPC} values, on the other hand, still represent a weighted average, which hardly changes in the presence of the diruthenium-complexes, since DHPC (28 mM) in the mixtures is present in large excess as compared to **1-3** (1 mM).

Analogous experiments were performed using DHPC well below CMC (10 mM). A decrease in $D^{Ru\ complex}$ was also observed clearly for **1** and **2**, but no significant changes were observed for **3** (Figure S26). The extent of the changes in $D^{Ru\ complex}$ for **1** and **2** was, however, smaller than that observed when using DHPC above CMC. This indicates that the diruthenium complexes either also interact with DHPC monomers forming larger hetero-associates or that they lower the CMC of DHPC and promote the formation of micelles[57] even at lower DHPC concentration. In any case, the DOSY data demonstrate that **1** and **2** exhibit a pronounced affinity for interacting with the phospholipids, thereby enhancing their solubility.

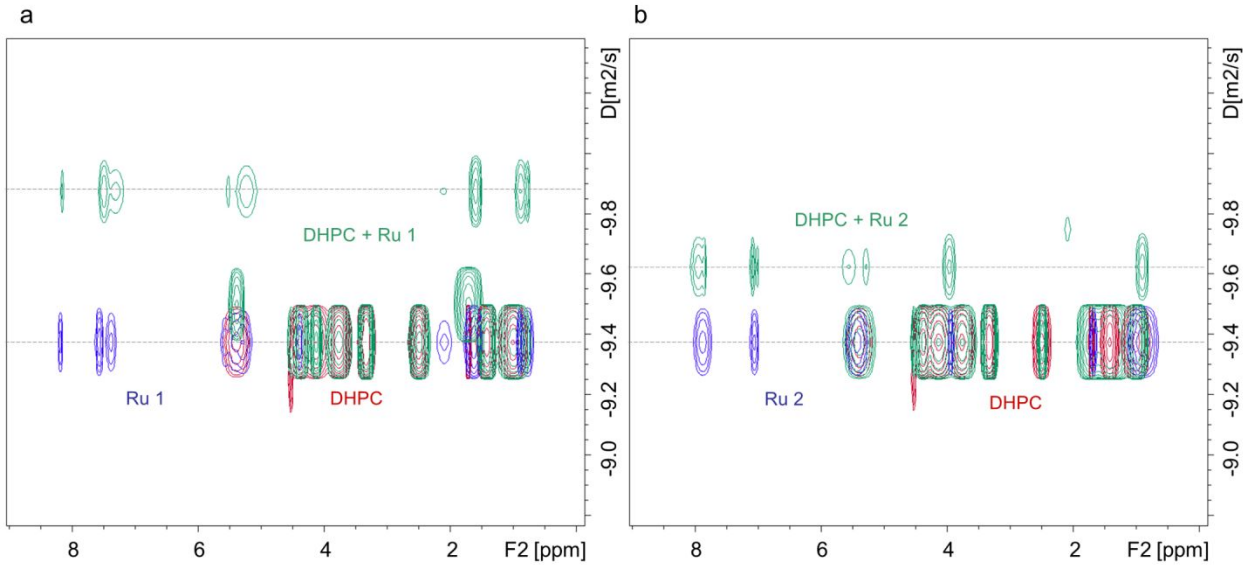

Figure 5. Overlay of DOSY spectra of (a): **1** (1 mM; blue), DHPC (28 mM; red) or mixture of both (green), respectively, dissolved in PBS (50 mM) / DMSO 4:1; (b): **2** (1 mM; blue), DHPC (28 mM; red) or mixture of both (green), respectively, dissolved in PBS (50 mM) / DMSO 4:1.

T_1 and T_2 relaxation: (i) Diruthenium complexes: When measuring the spin-lattice relaxation time (T_1), a significant decrease in T_1 was observed for several protons of complexes **1-3** when mixed with DOPC vesicles as can be seen in Figure S27. In the codissolution experiments, a similar tendency was observed but to a slightly smaller extent. Only relatively small changes (mainly slight decrease) in T_1 relaxation times were observed in complexes **1-3** in the presence of DHPC micelles (Figure S27).

(ii) DOPC: In the case of DOPC, a small decrease in T_1 was observed for the protons of the phospholipid choline residue as well as of the aliphatic chain in the presence of **1-3** (Figure S28). Very similar results were observed for DOPC from the codissolution experiment with **1-3** (Figure S29).

(iii) DHPC: DHPC protons also showed a decrease in T_1 in the presence of **1-2** and to a smaller extent also when mixed with **3**. Interestingly and in contrast to DOPC vesicles, the protons of the aliphatic chain of DHPC were more affected (Figure S28) as compared to the choline head.

While we observed a decrease of the T_1 relaxation times, the relation between T_1 and τ_c is not straightforward, since the variation of T_1 as a function of τ_c is parabolic, and the experimental determination of the minimum is demanding.[58]

The measurement of the T_2 relaxation times is, therefore, an important complement since T_2 decreases with increasing τ_c monotonously.

As compared to T_1, the observed decrease in T_2 relaxation times of all selected protons of complexes **1-3** in the presence of DHPC micelles was more consistent. When **1-3** were

present in suspension with DOPC vesicles, T_2 decreased significantly by about a factor ten for most of the protons (Figure 6).

Similar to T_1, the T_2 values of DHPC slightly dropped in the presence of the diruthenium complexes **1-3** (Figure 7). The decrease was slightly more pronounced with complex **2**. For DOPC vesicles present in suspension with **1-3**, the T_2 values of the choline dropped clearly while those of the lipid chain were only slightly affected (Figure 7). We have noticed similar results for the codissolution samples (Figure S30).

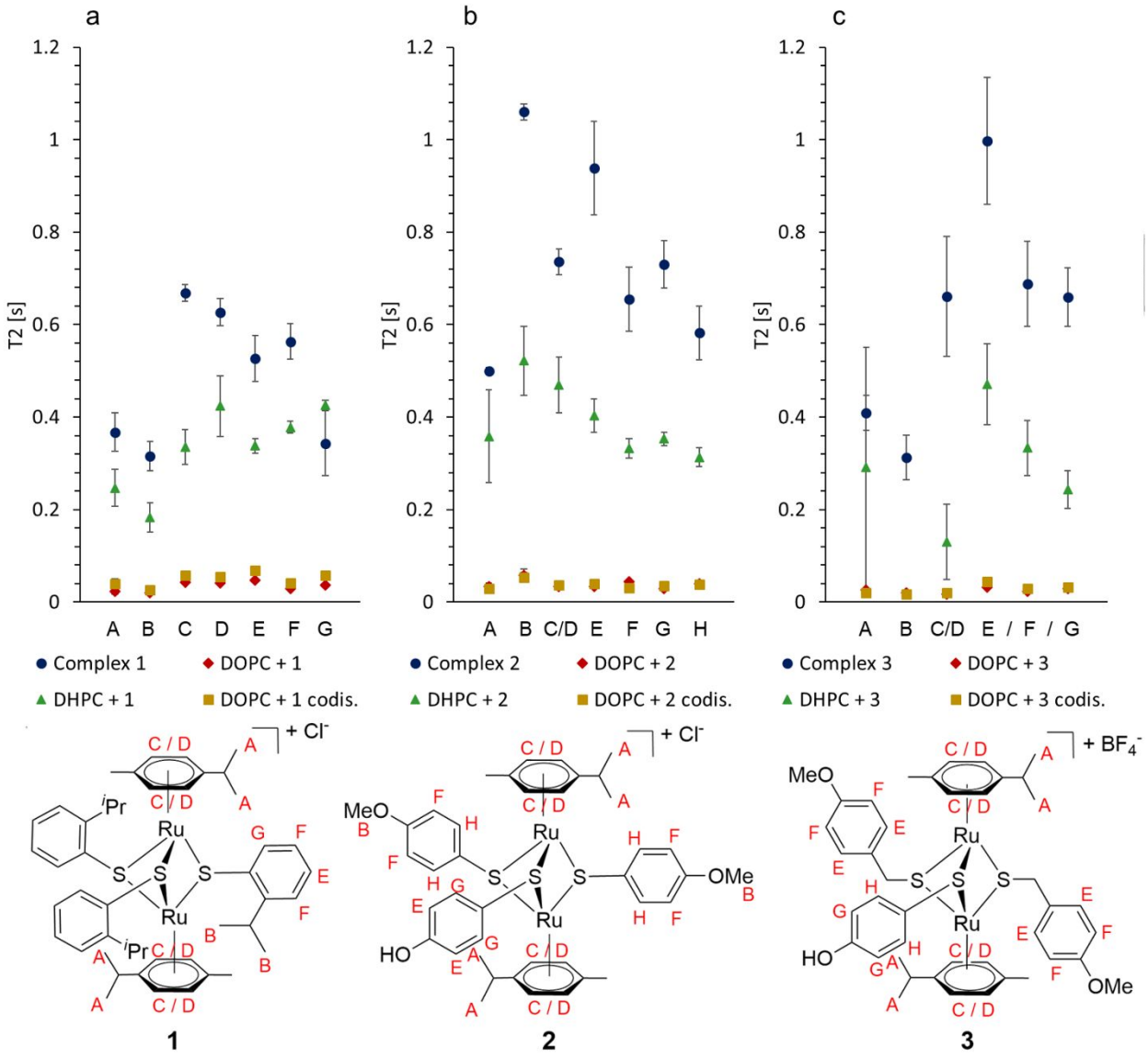

Figure 6. T_2 relaxation time of (a): **1** (1 mM) protons; (b): **2** (1 mM) protons; (c): **3** (1 mM) protons the in presence of DOPC (10 mM) vesicles or DHPC (28 mM) micelles, respectively, in PBS (50 mM)/DMSO. Only results for resonances with no overlap with phospholipid signals shown. Due to insufficient S/N it was not possible to determine T_2 of *p*-cymene methyl protons in case of **3** in mixture with DHPC.

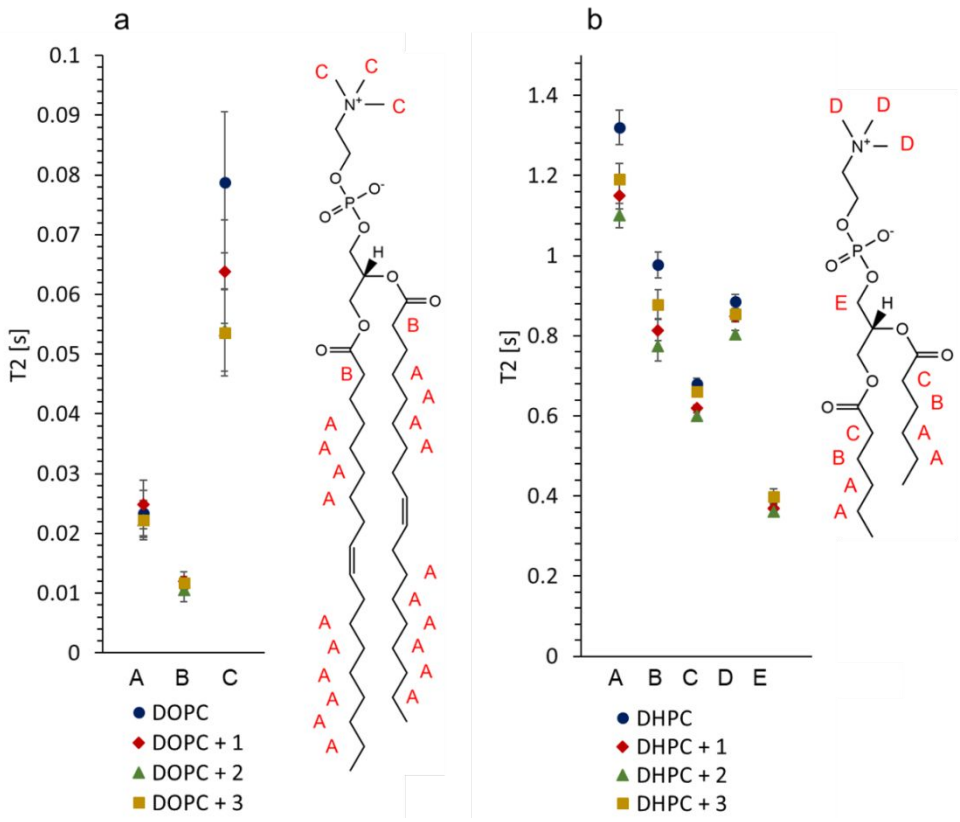

Figure 7. T_2 relaxation time of (a): DOPC (10 mM) vesicles or (b): DHPC (28 mM) micelles, respectively, in the presence of **1**, **2** and **3**, in PBS (50 mM)/DMSO. Only results for resonances with no overlap with signals of the complexes shown.

Putting the relaxation data together strongly suggest an interaction of the diruthenium complexes **1-3** with the DOPC vesicles. Furthermore, it is likely that the diruthenium complexes **1-3** are located on the surface of the phospholipid bilayer since the T_2

relaxation time of the choline residue in DOPC vesicles is the most affected in the presence of **1-3**.

Likewise, the drop of the T_2 values of DHPC in the presence of the diruthenium complexes **1-3** also points to an interaction between DHPC and **1-3**. In this case, the decrease in T_2 was observed for β-CH_2, γ/δ-CH_2 and to a smaller extent also for the N-methyl protons. The extent of the reduction in T_2 was thus selective and therefore not solely caused by a decrease in the overall tumbling of the micelles. Local restriction in mobility of the corresponding chain segments through interaction with the complex is most likely responsible for the observed drop in T_2. However, changes in the local orientation or order of the segments and consequently their solvent exposure may also contribute here.

The codissolution of the diruthenium complexes with DOPC prior to vesicle formation did not significantly change the relaxation times of the protons considered when compared to the procedure of adding the complexes to preformed vesicles in solution.

Lanthanide shift experiments: The paramagnetic lanthanide ion Pr^{3+} in solution is long known and used for inducing chemical shift changes and line broadening of NMR resonances of nuclei in

close proximity, thus enabling the identification of coordination atoms or binding pockets for proteins and enzymes.[59] Since Pr^{3+} does not penetrate phospholipid bilayers,[60] it will induce chemical shift change and line broadening only for the nuclei of the outer phospholipid layer, allowing to distinguish interior and exterior of a vesicle as can be seen in ^{31}P NMR spectra of DOPC vesicles (Figure 8). The resonance of the phosphocholine head groups exposed to the exterior solution where $PrCl_3$ is present is shifted by about 12.3 ppm downfield as compared to the unperturbed resonance. Therefore, the phosphocholine signals that show no shift can be attributed to the interior layer of the vesicles where no Pr^{3+} is present. When both **1** and $PrCl_3$ are present in solution, the difference in the ^{31}P shift is only about 5.6 ppm indicating that some of the surface is already occupied by (also positively charged) **1**. With this experiment, we cannot however, exclude that **1** is also present inside the DOPC vesicle.

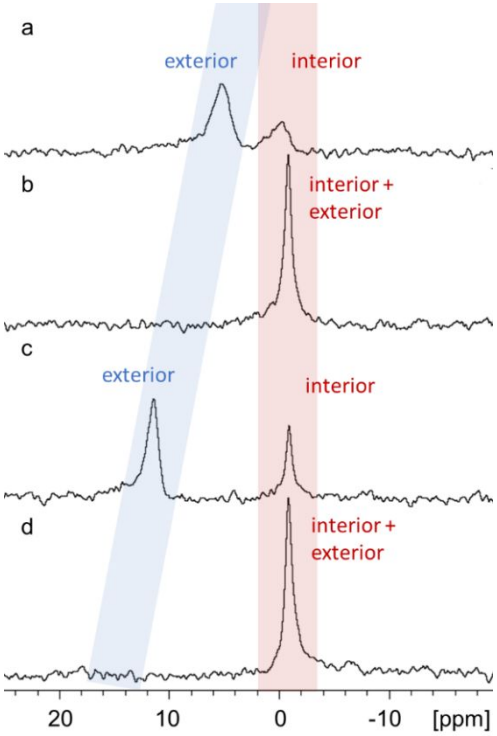

Figure 8. ^{31}P NMR of (a): DOPC (10 mM) vesicles and **1** (1 mM) in presence of 1 mM $PrCl_3$ in D_2O/DMSO, (b): DOPC (10 mM) and **1** (1 mM) in D_2O/DMSO, (c): DOPC (10 mM) vesicles and $PrCl_3$ (1 mM) in D_2O/DMSO, (d): DOPC (10 mM) vesicles in D_2O/DMSO.

^1H NMR spectra showed similar results (Figure 9) - the resonances of the N-methyl protons were split and shifted in the presence of Pr^{3+} (Figure 9b). Additionally, a shoulder was observed for the N-methyl protons of the inner layer at 3.33 ppm in the presence of Pr^{3+} (Figure 9b), which might be caused by the polydispersity of the vesicles.

Interestingly, when both Pr^{3+} and **1** were present, the shoulder of the N-methyl protons of the inner layer disappeared, and a new splitting of the N-methyl protons belonging to the exterior layer was observed (Figure 9d). This could be due to some of the exterior choline heads being exposed to Pr^{3+} while others being influenced by both **1** and Pr^{3+} together.

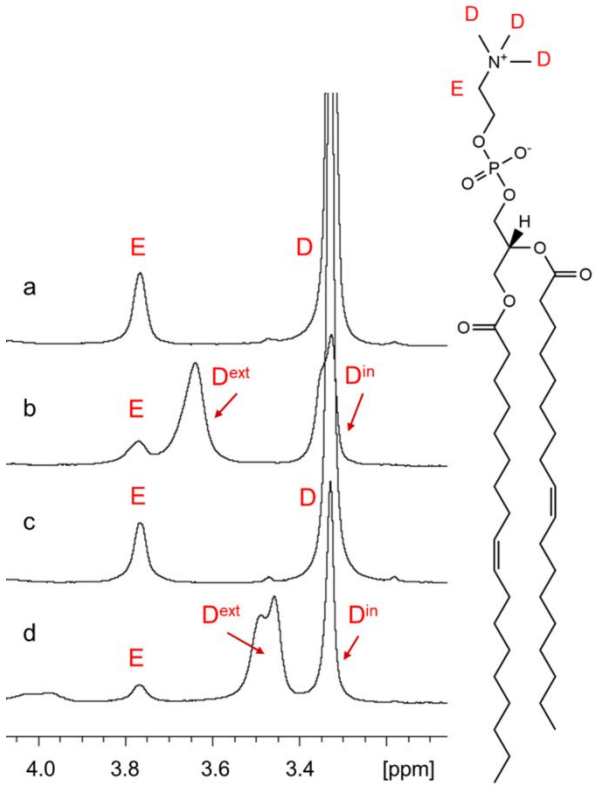

Figure 9. ^{1}H NMR of (a): DOPC (10 mM) vesicles in D_2O/DMSO, (b): DOPC (10 mM) vesicles in presence of 1 mM $PrCl_3$ in D_2O/DMSO, (c): DOPC (10 mM) vesicles and **1** (1 mM) in D_2O/DMSO, (d): DOPC (10 mM) vesicles, **1** (1 mM) and $PrCl_3$ (1 mM) in D_2O/DMSO.

Membrane passage: DOPC and a number of other phospholipids commonly used for model studies are zwitterionic. Nevertheless, the surface of zwitterionic phospholipid vesicles tends to be negatively charged, presumably due to the cationic N-methyl choline moiety being surrounded by anions in suspension.[61,62] Negative surface charge can

attract cationic diruthenium complexes towards DOPC vesicles. This is in line with what we have observed in our NMR study – the diruthenium complexes seem to be located close to the surface.

1-3 are intermediate/large sized cations possessing a nearly spherical shape, their charge is balanced by Cl^- or BF_4^- counterions, respectively. Hydrophobic cations are known to be able to permeate lipid bilayers[63] which has been observed not only for organic cations, but also for metal complexes.[64] The negative electric potential inside mitochondria is assumed to be a driving force for hydrophobic cations to enter the organelle.[14,65] This effect may be standing behind the diruthenium complex route to mitochondria.

CONCLUSIONS Lipophilicity of compounds is long known to influence the interactions with membranes and their passage, and thus it often controls the toxicity and efficacy of drugs. As previously established, symmetrical diruthenium complexes $[(\eta^6\text{-}p\text{-}MeC_6H_4Pr^i)_2Ru_2(R)_3]^+$ for which the calculated log *P* values of the individual thiol ligands range between 3.5-4.0 were those exhibiting the lowest IC_{50} values against cancer cells.[1,5]

We have evaluated the interactions of three diruthenium complexes with phospholipid membrane models using NMR spectroscopy. Based on 1D NMR spectra, ^{1}H and ^{31}P chemical shift changes, DOSY and relaxation data, we can conclude that the diruthenium complexes **1-3** interact with DOPC vesicles, especially the most water-soluble and lipophilic diruthenium complex **1**. Overall, the very high *in vitro* activity of **1** can be correlated to its ability to interact with the membrane as well as to its solubility. Importantly, the data also demonstrate that diruthenium complexes interact with phospholipids while maintaining their structural integrity. Both factors are important prerequisites for intracellular redistribution of the complexes among cell organelles such as mitochondria.

NOE and relaxation data indicated that the complexes are interacting with the choline headgroups and are located at the vesicle surface reaching into the membrane surface/water interface. The results obtained with **1** when Pr^{3+} was added suggest that the complex is located on the exterior of the vesicles. Taken all results together, we can conclude that the complexes most likely do not reside between the two phospholipid

layers and that - at least initially - membrane association in the head group region is most likely involving electrostatic interactions.

To some extent, the complexes also interacted with dynamic phospholipid species, as observed in the case of DHPC micelle/free phospholipid solutions. Additionally, the presence of the complexes in DHPC solutions below CMC induced the formation of micelles or aggregates. These studies indicated that the diruthenium complexes also exhibit a certain affinity for the phospholipid chain. However, dynamics of DOPC bilayer (together with hydrophobic effect) may be preventing fast passive transmembrane passage so that interactions with the membrane surface prevail.

There are certain limitations in our study that need to be considered. While DMSO is a common co-solvent for drug in vitro studies, it can cause membrane perturbations and is known to form clusters with water and in this way could have an influence in our study as well. Further, while the phospholipid-complex mixtures remain stable in terms of NMR-experiments, leakage from the vesicles cannot be excluded.

In summary, the data suggest that diruthenium complexes are probably not only entering cells by passive diffusion, and that additional uptake mechanisms are likely

involved. Recently, affinity chromatography using extracts from *T. gondii*-infected human fibroblasts led to the identification of TgEF1 as well as its human homologue as major targets of the similar, highly *in vitro* active complex $[(\eta^6\text{-}p\text{-}MeC_6H_4Pr^i)_2Ru_2(R^1)_2(R^2)]^+$ (R^1 = SC_6H_4-*p*-Bu^t, R^2 = SC_6H_4-*p*-OH) and various other host proteins were found to bind to this as well.[10]

In the context of recent findings using ICP-MS showing a significant amount of ruthenium present within mitochondria of treated cells and parasites,[5,10] and that the apoptotic event in cancer cells treated with $[(\eta^6\text{-}p\text{-}MeC_6H_4Pr^i)_2Ru_2(R)_3]^+$ (R = SC_6H_4-*p*-Bu^t) was confirmed by the decrease in the mitochondrial membrane potential ($\Delta\psi_m$),[66] the following mechanism appears plausible: the cationic lipophilic complex enters the cell or the parasite and targets mitochondria attracted by their negative potential. Subsequently, it passes through the outer mitochondrial membrane, and (a) remains adsorbed to the outer surface of the inner membrane or (b) remains in the intermembrane space and perturbs the electron transport chain. It appears less probable that the diruthenium complexes enter the mitochondrial matrix, since the inner membrane does not contain

porins, and all molecules require special membrane transporters to enter or exit the matrix.

In order to get more insights into the exact targets and mechanisms of action(s) of diruthenium complexes, further studies will be required, possibly involving membrane potential or specific uptake inhibitors and stripping off the outer mitochondrial membrane. The knowledge will aid further development and optimization of efficient diruthenium complexes as potential anti-cancer and antiparasitic drugs.

ASSOCIATED CONTENT

Supporting Information. Figures S1-2: DOSY-based CMC estimation. Figure S3: ^{1}H NMR of DHPC with concentrations varied. Figures S4-6: NOE spectra. Figures S7-8: DOSY fitting plots for DOPC and DHPC. Figure S9: DLS. Table S1-3: Chemical shift changes in the presence of phospholipids. Figure S10: ^{1}H NMR DOPC assignment. Figure S11: ^{1}H NMR DHPC assignment. Figures S12-14: ^{1}H NMR of **1-3** in the presence of DOPC. Figures S15-17 ESI-MS. Figures S18-20: ^{1}H NMR of **1-3** in the presence of DHPC. Figure S21: ^{31}P NMR spectra. Figure S22: DOSY of **3** in the

presence of DOPC. Figure S23: **2** codissolution with DOPC. Figure S24: ^{1}H NMR of DOPC codissolved with **1-3**. Figure S25: DOSY of **3** in the presence of DHPC. Figure S26: DOSY of sub-CMC DHPC in the presence of **1-3**. Figure S27: T_1 relaxation of **1-3** in presence of DOPC and DHPC. Figure S28: T_1 relaxation of DOPC and DHPC in presence of **1-3**. Figure S29: T_1 relaxation of DOPC codissolved with **1-3**. Figure S30: T_2 relaxation of DOPC codissolved with **1-3**.

The following files are available free of charge.

Supporting information (PDF)

AUTHOR INFORMATION

Corresponding Authors

*julien.furrer@dcb.unibe.ch; Tel.: +41 31 631 4383

*martina.vermathen@dcb.unibe.ch; Tel.: +41 31 631 3948

*hedvika.primasova@dcb.unibe.ch; Tel.: +41 31 631 4384

Author Contributions

The manuscript was written through contributions of all authors. All authors have given approval to the final version of the manuscript.

ACKNOWLEDGMENT

We are very grateful to Lisa Rahnfeld and Paola Luciani of the Department of Chemistry and Biochemistry, University of Bern for the viscosity measurement, for introducing us to their DLS device and letting us use it. The authors acknowledge financial support from the University of Bern.

ABBREVIATIONS

CMC critical micelle concentration, COSY correlation spectroscopy, CPMG Carr-Purcell-Meiboom-Gill, DHPC 1,2-dihexanoyl-*sn*-glycero-3-phosphocholine, DLS dynamic light scattering, DMSO dimethyl sulfoxide, DOPC 1,2-dioleoyl-*sn*-glycero-3-phosphocholine, DOSY diffusion ordered spectroscopy, HMBC heteronuclear multiple bond correlation (spectroscopy), HSQC heteronuclear single quantum coherence (spectroscopy), ICP-MS inductively coupled plasma mass spectrometry, MS mass spectrometry, NMR nuclear magnetic resonance (spectroscopy), NOE nuclear

Overhauser effect, PBS phosphate-buffered saline, PDI polydispersity index, ROS reactive oxygen species, TEM transmission electron microscopy.

REFERENCES

(1) Furrer, J.; Süss-Fink, G. Thiolato-Bridged Dinuclear Arene Ruthenium Complexes and Their Potential as Anticancer Drugs. *Coord. Chem. Rev.* **2016**, *309*, 36–50. https://doi.org/10.1016/j.ccr.2015.10.007.

(2) Giannini, F.; Geiser, L.; Paul, L. E. H.; Roder, T.; Therrien, B.; Süss-Fink, G.; Furrer, J. Tuning the in Vitro Cell Cytotoxicity of Dinuclear Arene Ruthenium Trithiolato Complexes: Influence of the Arene Ligand. *J. Organomet. Chem.* **2015**, *783*, 40–45. https://doi.org/10.1016/j.jorganchem.2015.02.010.

(3) Giannini, F.; Paul, L. E. H.; Furrer, J.; Therrien, B.; Süss-Fink, G. Highly Cytotoxic Diruthenium Trithiolato Complexes of the Type [(H6-p-MeC6H4Pri)2Ru2(M2-SR)3]+: Synthesis, Characterization, Molecular Structure and in Vitro Anticancer Activity. *New J. Chem.* **2013**, *37* (11), 3503. https://doi.org/10.1039/c3nj00476g.

(4) Primasová; Paul; Diserens; Primasová; Vermathen; Vermathen; Furrer. 1H HR-

MAS NMR-Based Metabolomics of Cancer Cells in Response to Treatment with the Diruthenium Trithiolato Complex [(p-MeC6H4iPr)2Ru2(SC6H4-p-But)3]+ (DiRu-1). *Metabolites* **2019**, *9* (7), 146. https://doi.org/10.3390/metabo9070146.

(5) Basto, A. P.; Anghel, N.; Rubbiani, R.; Müller, J.; Stibal, D.; Giannini, F.; Süss-Fink, G.; Balmer, V.; Gasser, G.; Furrer, J.; et al. Targeting of the Mitochondrion by Dinuclear Thiolato-Bridged Arene Ruthenium Complexes in Cancer Cells and in the Apicomplexan Parasite Neospora Caninum. *Metallomics* **2019**, *11*, 462–474. https://doi.org/10.1039/c8mt00307f.

(6) Tomšík, P.; Muthná, D.; Řezáčová, M.; Mičuda, S.; Ćmielová, J.; Hroch, M.; Endlicher, R.; Červinková, Z.; Rudolf, E.; Hann, S.; et al. [(P-MeC6H4Pri)2Ru2(SC6H4-p-But)3]Cl (Diruthenium-1), a Dinuclear Arene Ruthenium Compound with Very High Anticancer Activity: An in Vitro and in Vivo Study. *J. Organomet. Chem.* **2015**, *782*, 42–51. https://doi.org/10.1016/j.jorganchem.2014.10.050.

(7) Koceva-Chyła, A.; Matczak, K.; Hikisz, M. P.; Durka, M. K.; Kochel, M. K.; Süss-

Fink, G.; Furrer, J.; Kowalski, K. Insights into the in Vitro Anticancer Effects of Diruthenium-1. *ChemMedChem* **2016**, *2*, 2171–2187. https://doi.org/10.1002/cmdc.201600315.

(8) Muthná, D.; Tomšík, P.; Havelek, R.; Köhlerová, R.; Kasilingam, V.; Čermáková, E.; Stíbal, D.; Řezáčová, M.; Süss-Fink, G. In-Vitro and in-Vivo Evaluation of the Anticancer Activity of Diruthenium-2, a New Trithiolato Arene Ruthenium Complex [(H6-p-MeC6H4Pri)2Ru2(μ-S-p-C6H4OH)3]Cl. *Anticancer. Drugs* **2016**, *27* (7), 643–650. https://doi.org/10.1097/CAD.0000000000000374.

(9) Giannini, F.; Süss-Fink, G.; Furrer, J. Efficient Oxidation of Cysteine and Glutathione Catalyzed by a Dinuclear Areneruthenium Trithiolato Anticancer Complex. *Inorg. Chem.* **2011**, *50* (21), 10552–10554. https://doi.org/10.1021/ic201941j.

(10) Basto, A. P.; Müller, J.; Rubbiani, R.; Stibal, D.; Giannini, F.; Süss-Fink, G.; Balmer, V.; Hemphill, A.; Gasser, G.; Furrer, J. Characterization of the Activities of Dinuclear Thiolato-Bridged Arene Ruthenium Complexes against Toxoplasma Gondii.

Antimicrob. Agents Chemother. **2017**, *61* (9), e01031-17.

(11) Shinoda, W. Permeability across Lipid Membranes. *Biochim. Biophys. Acta - Biomembr.* **2016**, *1858* (10), 2254–2265. https://doi.org/10.1016/j.bbamem.2016.03.032.

(12) Missner, A.; Pohl, P. 110 Years of the Meyer-Overton Rule: Predicting Membrane Permeability of Gases and Other Small Compounds. *ChemPhysChem* **2009**, *10*, 1405–1414.

(13) Bourgaux, C.; Couvreur, P. Interactions of Anticancer Drugs with Biomembranes: What Can We Learn from Model Membranes? *J. Control. Release* **2014**, *190*, 127–138. https://doi.org/10.1016/j.jconrel.2014.05.012.

(14) Liberman, E. A.; Topaly, V. P.; Tsofina, L. M.; Jasaitis, A. A.; Skulachev, V. P. Mechanism of Coupling of Oxidative Phosphorylation and the Membrane Potential of Mitochondria. *Nature* **1969**, *222*, 1076–1078.

(15) Murphy, M. P. Targeting Lipophilic Cations to Mitochondria. *Biochim. Biophys. Acta*

- *Bioenerg.* **2008**, *1777* (7–8), 1028–1031. https://doi.org/10.1016/j.bbabio.2008.03.029.

(16) Gasser, G.; Metzler-Nolte, N. The Potential of Organometallic Complexes in Medicinal Chemistry. *Curr. Opin. Chem. Biol.* **2012**, *16* (1–2), 84–91. https://doi.org/10.1016/j.cbpa.2012.01.013.

(17) Giannini, F.; Furrer, J.; Ibao, A. F.; Süss-Fink, G.; Therrien, B.; Zava, O.; Baquie, M.; Dyson, P. J.; Štěpnička, P. Highly Cytotoxic Trithiophenolatodiruthenium Complexes of the Type [(H6-p-MeC6H4Pr i) 2Ru2(SC6H4-p-X)3] +: Synthesis, Molecular Structure, Electrochemistry, Cytotoxicity, and Glutathione Oxidation Potential. *J. Biol. Inorg. Chem.* **2012**, *17* (6), 951–960. https://doi.org/10.1007/s00775-012-0911-2.

(18) Deleu, M.; Crowet, J. M.; Nasir, M. N.; Lins, L. Complementary Biophysical Tools to Investigate Lipid Specificity in the Interaction between Bioactive Molecules and the Plasma Membrane: A Review. *Biochim. Biophys. Acta - Biomembr.* **2014**, *1838* (12), 3171–3190. https://doi.org/10.1016/j.bbamem.2014.08.023.

(19) Alves, A. C.; Ribeiro, D.; Nunes, C.; Reis, S. Biophysics in Cancer: The Relevance of Drug-Membrane Interaction Studies. *Biochim. Biophys. Acta - Biomembr.* **2016**, *1858* (9), 2231–2244. https://doi.org/10.1016/j.bbamem.2016.06.025.

(20) Peetla, C.; Stine, A.; Labhasetwar, V. Biophysical Interactions with Model Lipid Membranes: Applications in Drug Discovery and Drug Delivery. *Mol. Pharm.* **2009**, *6* (5), 1264–1276. https://doi.org/10.1021/mp9000662.

(21) Clark, T. D.; Bartolotti, L.; Hicks, R. P. The Application of DOSY NMR and Molecular Dynamics Simulations to Explore the Mechanism(s) of Micelle Binding of Antimicrobial Peptides Containing Unnatural Amino Acids. *Biopolymers* **2013**, *99* (8), 548–561. https://doi.org/10.1002/bip.22215.

(22) McBain, J. W.; Salmon, C. S. Colloidal Electrolytes. Soap Solutions and Their Constitution. *J. Am. Chem. Soc.* **1920**, *42* (3), 426–460. https://doi.org/10.1021/ja01448a010.

(23) Brand, T.; Cabrita, E. J.; Berger, S. Intermolecular Interaction as Investigated by

NOE and Diffusion Studies. *Prog. Nucl. Magn. Reson. Spectrosc.* **2005**, *46* (4), 159–196. https://doi.org/10.1016/j.pnmrs.2005.04.003.

(24) Vermathen, M.; Vermathen, P.; Simonis, U.; Bigler, P. Time-Dependent Interactions of the Two Porphyrinic Compounds Chlorin E6 and Mono-L-Aspartyl-Chlorin E6 with Phospholipid Vesicles Probed by NMR Spectroscopy. *Langmuir* **2008**, *24* (21), 12521–12533. https://doi.org/10.1021/la802040v.

(25) Jensen, M.; Bjerring, M.; Nielsen, N. C.; Nerdal, W. Cisplatin Interaction with Phosphatidylserine Bilayer Studied by Solid-State NMR Spectroscopy. *J. Biol. Inorg. Chem.* **2010**, *15* (2), 213–223. https://doi.org/10.1007/s00775-009-0586-5.

(26) Crans, D. C.; Rithner, C. D.; Baruah, B.; Gourley, B. L.; Levinger, N. E. Molecular Probe Location in Reverse Micelles Determined by NMR Dipolar Interactions. *J. Am. Chem. Soc.* **2006**, *128* (13), 4437–4445. https://doi.org/10.1021/ja0583721.

(27) Scheidt, H. A.; Huster, D. The Interaction of Small Molecules with Phospholipid Membranes Studied by 1H NOESY NMR under Magic-Angle Spinning. *Acta*

Pharmacol. Sin. **2008**, *29* (1), 35–49. https://doi.org/10.1111/j.1745-7254.2008.00726.x.

(28) Vermathen, M.; Marzorati, M.; Vermathen, P.; Bigler, P. PH-Dependent Distribution of Chlorin E6 Derivatives across Phospholipid Bilayers Probed by NMR Spectroscopy. *Langmuir* **2010**, *26* (13), 11085–11094. https://doi.org/10.1021/la100679y.

(29) Marzorati, M.; Bigler, P.; Vermathen, M. Interactions between Selected Photosensitizers and Model Membranes: An NMR Classification. *Biochim. Biophys. Acta - Biomembr.* **2011**, *1808* (6), 1661–1672. https://doi.org/10.1016/j.bbamem.2011.02.011.

(30) Vermathen, M.; Marzorati, M.; Bigler, P. Self-Assembling Properties of Porphyrinic Photosensitizers and Their Effect on Membrane Interactions Probed by NMR Spectroscopy. *J. Phys. Chem. B* **2013**, *117* (23), 6990–7001. https://doi.org/10.1021/jp403331n.

(31) Li, H.; Zhao, T.; Sun, Z. Analytical Techniques and Methods for Study of Drug-Lipid Membrane Interactions. *Rev. Anal. Chem.* **2018**, *37* (1), 1–23. https://doi.org/10.1515/revac-2017-0012.

(32) Söderman, O.; Stilbs, P. NMR Studies of Complex Surfactant Systems. *Prog. Nucl. Magn. Reson. Spectrosc.* **1994**, *26* (PART 5), 445–482. https://doi.org/10.1016/0079-6565(94)80013-8.

(33) Stíbal, D.; Therrien, B.; Süss-Fink, G.; Nowak-Sliwinska, P.; Dyson, P. J.; Čermáková, E.; Řezáčová, M.; Tomšík, P. Chlorambucil Conjugates of Dinuclear P-Cymene Ruthenium Trithiolato Complexes: Synthesis, Characterization and Cytotoxicity Study in Vitro and in Vivo. *J. Biol. Inorg. Chem.* **2016**, *21* (4), 443–452. https://doi.org/10.1007/s00775-016-1353-z.

(34) Stibal, D. Thiolato-Bridged Arene Ruthenium Complexes as Anticancer Agents, Université de Neuchâtel, 2015.

(35) Söderman, O.; Stilbs, P.; Price, W. S. NMR Studies of Surfactants. *Concepts Magn.*

Reson. Part A Bridg. Educ. Res. **2004**, *23* (2), 121–135. https://doi.org/10.1002/cmr.a.20022.

(36) Schick, M. J. Effect of Temperature on the Critical Micelle Concentration of Nonionic Detergents. Thermodynamics of Micelle Formation 1 . *J. Phys. Chem.* **2007**, *67* (9), 1796–1799. https://doi.org/10.1021/j100803a013.

(37) Dua, J. S.; Rana, A. C.; Bhandari, A. K. Liposomes - Methodology and Applications. *Int. J. Pharm. Stud. Res.* **2012**, *3*, 14–20.

(38) Stott, K.; Keeler, J.; Van, Q. N.; Shaka, A. J. One-Dimensional NOE Experiments Using Pulsed Field Gradients. *J. Magn. Reson.* **1997**, *125* (2), 302–324. https://doi.org/10.1006/jmre.1997.1110.

(39) Wu, D. H.; Chen, A.; Johnson, C. S. An Improved Diffusion-Ordered Spectroscopy Experiment Incorporating Bipolar-Gradient Pulses. *Journal of Magnetic Resonance, Series A*. 1995, pp 260–264. https://doi.org/10.1006/jmra.1995.1176.

(40) Stejskal, E. O.; Tanner, J. E. Spin Diffusion Measurements: Spin Echoes in the

Presence of a Time-Dependent Field Gradient. *J. Chem. Phys.* **1965**, *42* (1), 288–292. https://doi.org/10.1063/1.1695690.

(41) Carr, H. Y.; Purcell, E. M. Effects of Diffusion on Free Precession in Nuclear Magnetic Resonance Experiments. *Phys. Rev.* **1954**, *94* (3), 630–638.

(42) Meiboom, S.; Gill, D. Modified Spin-Echo Method for Measuring Nuclear Relaxation Times. *Rev. Sci. Instrum.* **1958**, *29* (8), 688–691. https://doi.org/10.1063/1.1716296.

(43) Gabriel, N. E.; Roberts, M. F. Spontaneous Formation of Stable Unilamellar Vesicles. *Biochemistry* **1984**, *23* (18), 4011–4015. https://doi.org/10.1021/bi00313a001.

(44) Giannini, F.; Furrer, J.; Süss-Fink, G.; Clavel, C. M.; Dyson, P. J. Synthesis, Characterization and in Vitro Anticancer Activity of Highly Cytotoxic Trithiolato Diruthenium Complexes of the Type [(H6-p-MeC6H4iPr)2Ru2(M2-SR1)2(M2-SR2)]+ Containing Different Thiolato Bridges. *J. Organomet. Chem.* **2013**, *744*, 41–

48. https://doi.org/10.1016/j.jorganchem.2013.04.049.

(45) Schreier, S.; Malheiros, S. V. P.; De Paula, E. Surface Active Drugs: Self-Association and Interaction with Membranes and Surfactants. Physicochemical and Biological Aspects. *Biochim. Biophys. Acta - Biomembr.* **2000**, *1508* (1–2), 210–234. https://doi.org/10.1016/S0304-4157(00)00012-5.

(46) Chou, J. J.; Baber, J. L.; Bax, A. Characterization of Phospholipid Mixed Micelles by Translational Diffusion. *J. Biomol. NMR* **2004**, *29* (3), 299–308. https://doi.org/10.1023/B:JNMR.0000032560.43738.6a.

(47) Björnerås, J.; Nilsson, M.; Mäler, L. Analysing DHPC/DMPC Bicelles by Diffusion NMR and Multivariate Decomposition. *Biochim. Biophys. Acta - Biomembr.* **2015**, *1848* (11), 2910–2917. https://doi.org/10.1016/j.bbamem.2015.09.002.

(48) Lin, T. L.; Chen, S. H.; Gabriel, N. E.; Roberts, M. F. Use of Small-Angle Neutron Scattering To Determine the Structure and Interaction of Dihexanoylphosphatidylcholine Micelles. *J. Am. Chem. Soc.* **1986**, *108* (12), 3499–

3507. https://doi.org/10.1021/ja00272a055.

(49) Lipfert, J.; Columbus, L.; Chu, X. V. B.; Lesley, S. A. Size and Shape of Detergent Micelles Determined by Small-Angle X-Ray Scattering. *J. Phys. Chem. B* **2007**, 12427–12438.

(50) Pianet, I.; André, Y.; Ducasse, M. A.; Tarascou, I.; Lartigue, J. C.; Pinaud, N.; Fouquet, E.; Dufourc, E. J.; Laguerre, M. Modeling Procyanidin Self-Association Processes and Understanding Their Micellar Organization: A Study by Diffusion NMR and Molecular Mechanics. *Langmuir* **2008**, *24* (19), 11027–11035. https://doi.org/10.1021/la8015904.

(51) Hughes, Z. E.; Mark, A. E.; Mancera, R. L. Molecular Dynamics Simulations of the Interactions of DMSO with DPPC and DOPC Phospholipid Membranes. *J. Phys. Chem. B* **2012**, *116* (39), 11911–11923. https://doi.org/10.1021/jp3035538.

(52) Šteflová, J.; Štefl, M.; Walz, S.; Knop, M.; Trapp, O. Comprehensive Study on Critical Micellar Concentrations of SDS in Acetonitrile-Water Solvents.

Electrophoresis **2016**, *37* (10), 1287–1295. https://doi.org/10.1002/elps.201500553.

(53) Zhou, Z.; Sayer, B. G.; Hughes, D. W.; Stark, R. E.; Epand, R. M. Studies of Phospholipid Hydration by High-Resolution Magic-Angle Spinning Nuclear Magnetic Resonance. *Biophys. J.* **1999**, *76* (1 I), 387–399. https://doi.org/10.1016/S0006-3495(99)77205-X.

(54) Fernández, C.; Hilty, C.; Wider, G.; Wüthrich, K. Lipid-Protein Interactions in DHPC Micelles Containing the Integral Membrane Protein OmpX Investigated by NMR Spectroscopy. *Proc. Natl. Acad. Sci. U. S. A.* **2002**, *99* (21), 13533–13537. https://doi.org/10.1073/pnas.212515099.

(55) Jeener, J.; Meier, B. H.; Bachmann, P.; Ernst, R. R. Investigation of Exchange Processes by Two-Dimensional NMR Spectroscopy. *J. Chem. Phys.* **1979**, *71* (11), 4546–4553. https://doi.org/10.1063/1.438208.

(56) Noggle, J. H.; Schirmer, R. E. *The Nuclear Overhauser Effect: Chemical*

Applications; Academic Press: New York, 1972.

(57) Akhter, M. S.; Alawi, S. M. The Effect of Organic Additives on Critical Micelle Concentration of Non-Aqueous Micellar Solutions. *Colloids Surfaces A Physicochem. Eng. Asp.* **2000**, *175* (3), 311–320. https://doi.org/10.1016/S0927-7757(00)00671-3.

(58) Ernst, R. R.; Bodenhausen, G.; Wokaun, A. *Principles of Nuclear Magnetic Resonance in One and Two Dimensions*; Oxford University Press: New York, 1994.

(59) Cockerill, A. F.; Davies, G. L. O.; Harden, R. C.; Rackham, D. M. Lanthanide Shift Reagents for Nuclear Magnetic Resonance Spectroscopy. *Chem. Rev.* **1973**, *73* (6), 553–588. https://doi.org/10.1021/cr60286a001.

(60) Wennerström, H.; Lindblom, G. Biological and Model Membranes Studied by Nuclear Magnetic Resonance of Spin One Half Nuclei. *Q. Rev. Biophys.* **1977**, *10* (1), 67–96.

(61) Claessens, M. M. A. E.; Van Oort, B. F.; Leermakers, F. A. M.; Hoekstra, F. A.;

Stuart, M. A. C. Charged Lipid Vesicles: Effects of Salts on Bending Rigidity, Stability, and Size. *Biophys. J.* **2004**, *87* (6), 3882–3893. https://doi.org/10.1529/biophysj.103.036772.

(62) Tatulian, S. A. Effect of Lipid Phase Transition on the Binding of Anions to Dimyristoylphosphatidylcholine Liposomes. *Biochim. Biophys. Acta* **1983**, *736* (2), 189–195. https://doi.org/10.1016/0005-2736(83)90283-3.

(63) Flewelling, R. F.; Hubbell, W. L. The Membrane Dipole Potential in a Total Membrane Potential Model. Applications to Hydrophobic Ion Interactions with Membranes. *Biophys. J.* **1986**, *49* (2), 541–552. https://doi.org/10.1016/S0006-3495(86)83664-5.

(64) Puckett, C. A.; Ernst, R. J.; Barton, J. K. Exploring the Cellular Accumulation of Metal Complexes. *Dalt. Trans.* **2010**, *39* (5), 1159–1170. https://doi.org/10.1039/b922209j.

(65) Rokitskaya, T. I.; Sumbatyan, N. V.; Tashlitsky, V. N.; Korshunova, G. A.;

Antonenko, Y. N.; Skulachev, V. P. Mitochondria-Targeted Penetrating Cations as Carriers of Hydrophobic Anions through Lipid Membranes. *Biochim. Biophys. Acta - Biomembr.* **2010**, *1798* (9), 1698–1706. https://doi.org/10.1016/j.bbamem.2010.05.018.

(66) Petruk, G.; Monti, D. M.; Ferraro, G.; Pica, A.; D'Elia, L.; Pane, F.; Amoresano, A.; Furrer, J.; Kowalski, K.; Merlino, A. Encapsulation of the Dinuclear Trithiolato-Bridged Arene Ruthenium Complex Diruthenium-1 in an Apoferritin Nanocage: Structure and Cytotoxicity. *ChemMedChem* **2019**, *14* (5), 594–602. https://doi.org/10.1002/cmdc.201800805.

TOC graphic

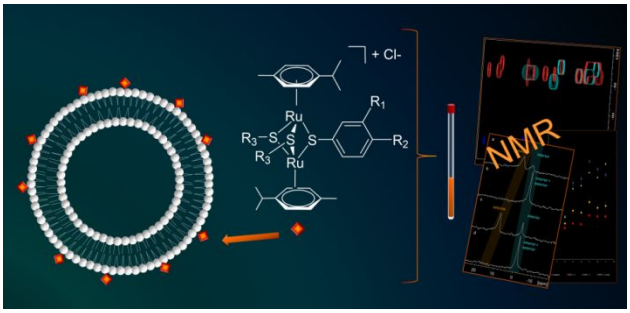

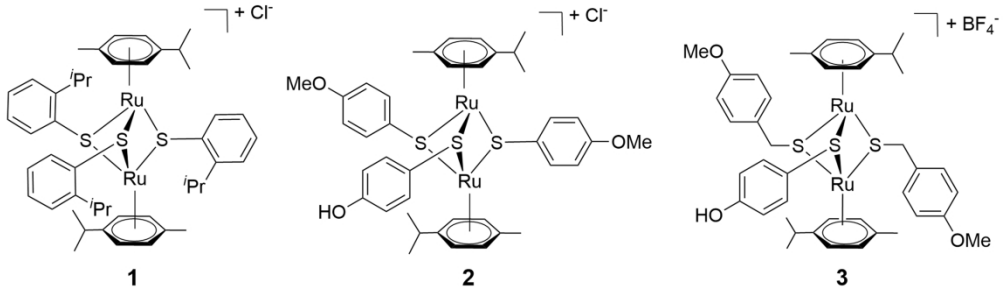

Figure 1. Structures of the three diruthenium complexes (1-3) investigated in this work.

165x49mm (600 x 600 DPI)

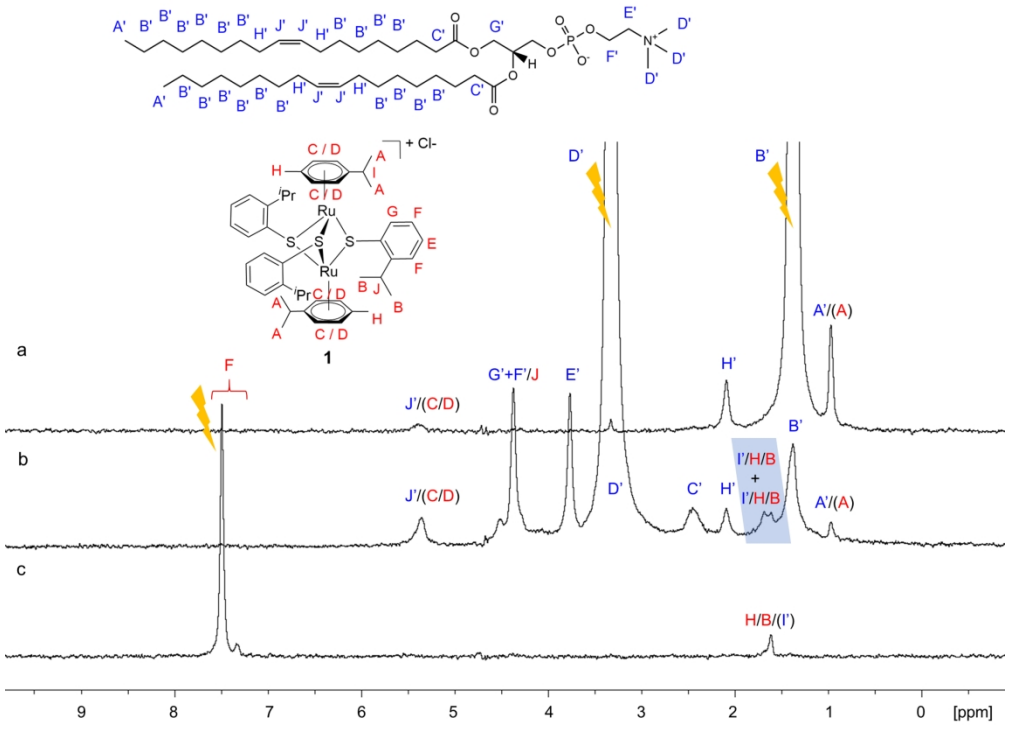

Figure 2. Superimposed 1D NOE NMR spectra of 1 (1 mM) and DOPC (10 mM) vesicles in PBS/DMSO. Irradiated (a): 1.367 ppm; (b): 3.328 ppm; (c): 7.494 ppm. Mixing time 100 ms, relaxation delay 1s, 2048 scans, 8192 TD data points, acquisition time 511 ms, spectral width 8012.8 Hz.

177x129mm (400 x 400 DPI)

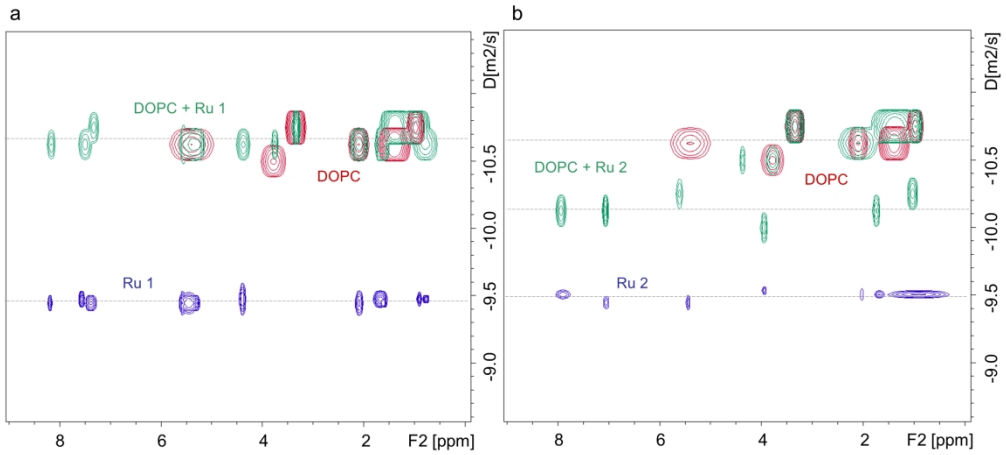

Figure 3. Overlay of DOSY spectra of (a): 1 (1 mM; blue), DOPC (10 mM; red) or mixture of both (green), respectively, dissolved in PBS (50 mM) / DMSO 4:1; (b): 2 (1 mM; blue), DOPC (10 mM; red) or mixture of both (green), respectively, dissolved in PBS (50 mM) / DMSO 4:1.

165x74mm (600 x 600 DPI)

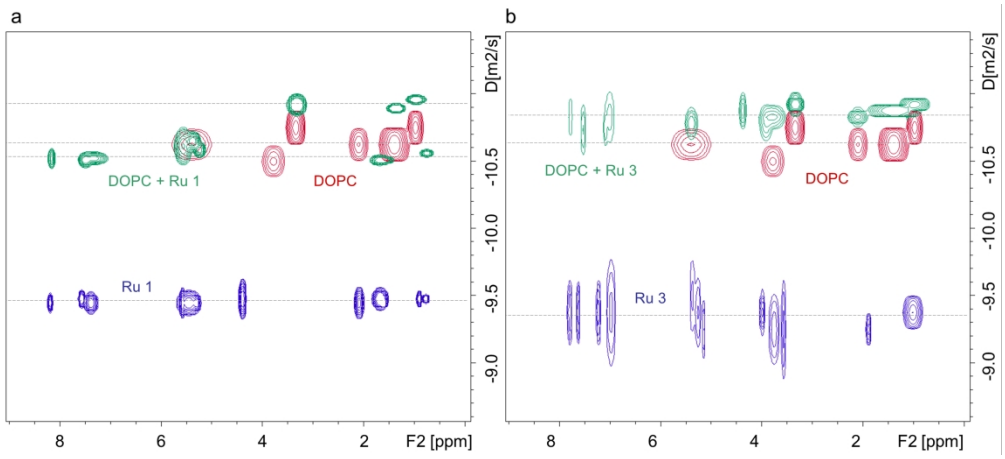

Figure 4. Overlay of DOSY spectra of (a): 1 (1 mM; blue), DOPC (10 mM; red) and 1 codissolved with DOPC upon vesicle formation in PBS (50 mM) / DMSO 4:1 (green); (b): 3 (1 mM; blue), DOPC (10 mM; red) and 3 codissolved with DOPC upon vesicle formation in PBS (50 mM) / DMSO 4:1 (green).

165x74mm (600 x 600 DPI)

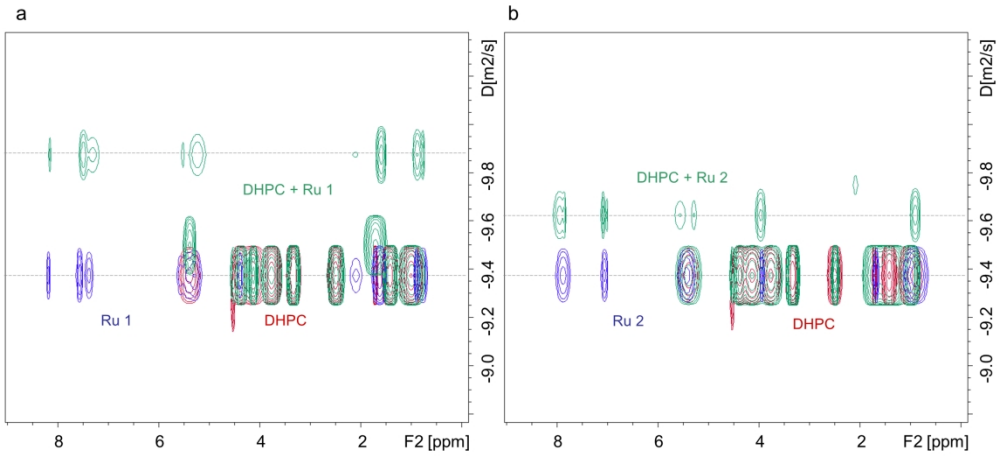

Figure 5. Overlay of DOSY spectra of (a): 1 (1 mM; blue), DHPC (28 mM; red) or mixture of both (green), respectively, dissolved in PBS (50 mM) / DMSO 4:1; (b): 2 (1 mM; blue), DHPC (28 mM; red) or mixture of both (green), respectively, dissolved in PBS (50 mM) / DMSO 4:1.

165x75mm (600 x 600 DPI)

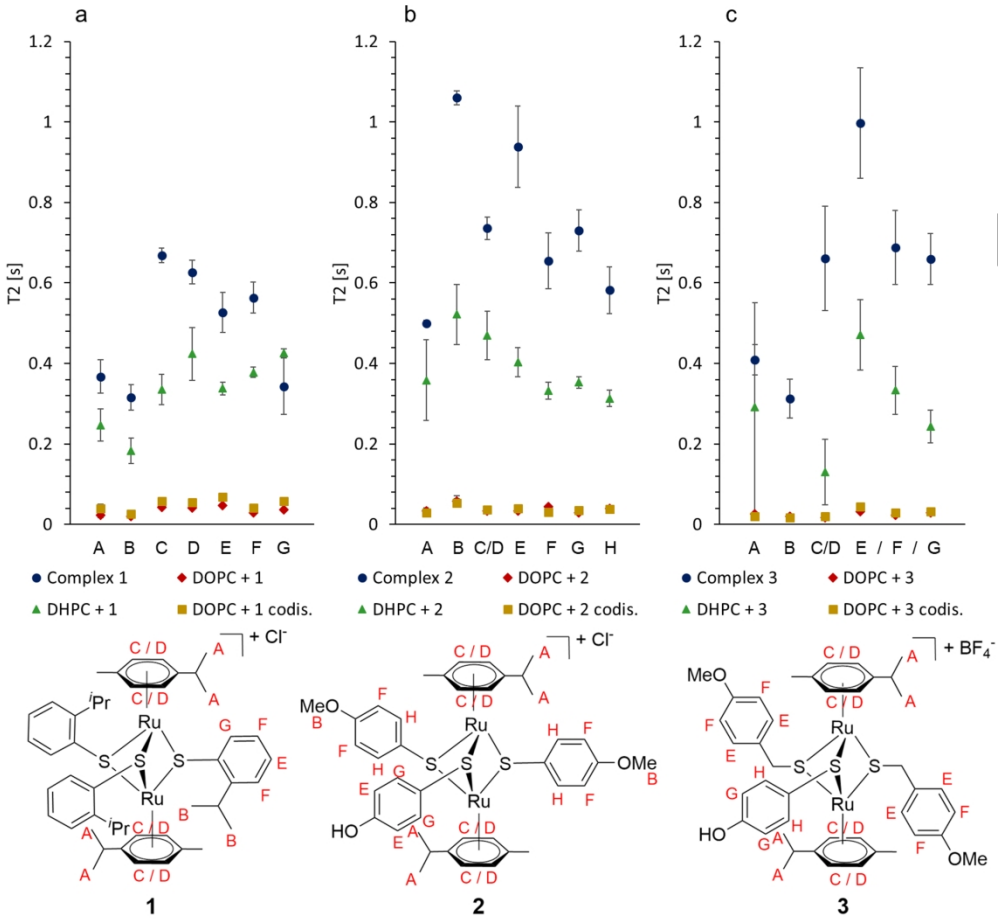

Figure 6. T2 relaxation time of (a): 1 (1 mM) protons; (b): 2 (1 mM) protons; (c): 3 (1 mM) protons the in presence of DOPC (10 mM) vesicles or DHPC (28 mM) micelles, respectively, in PBS (50 mM)/DMSO. Only results for resonances with no overlap with phospholipid signals shown. Due to insufficient S/N it was not possible to determine T2 of p-cymene methyl protons in case of 3 in mixture with DHPC.

165x152mm (500 x 500 DPI)

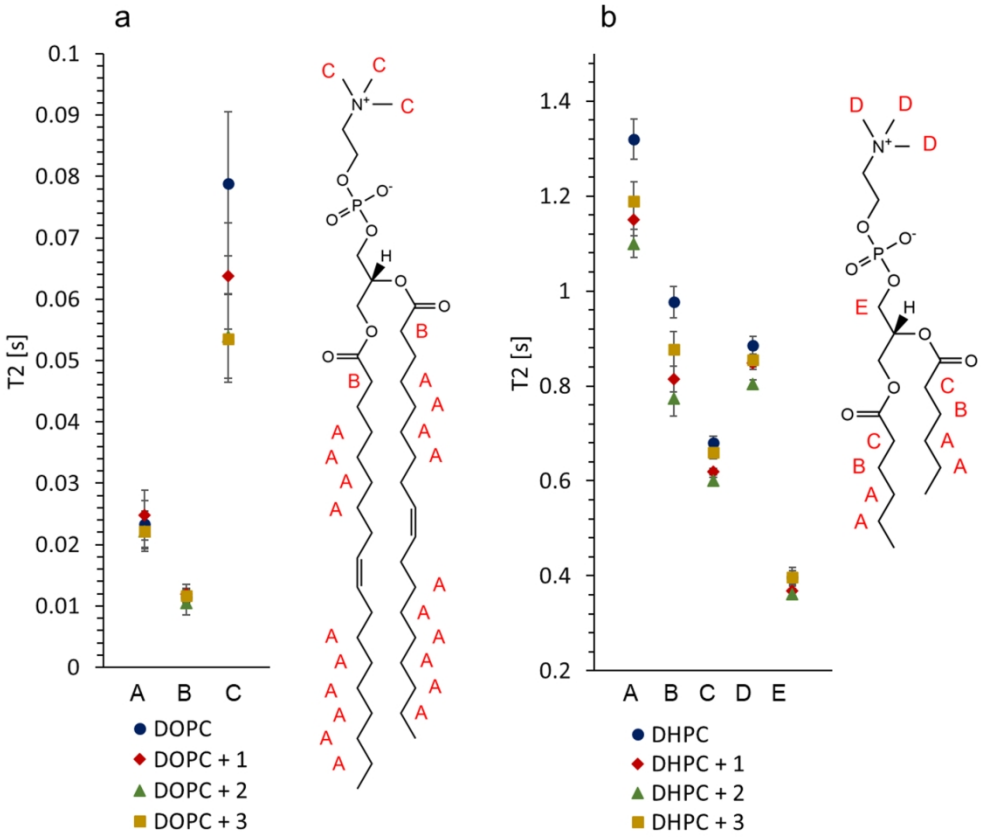

Figure 7. T2 relaxation time of (a): DOPC (10 mM) vesicles or (b): DHPC (28 mM) micelles, respectively, in the presence of 1, 2 and 3, in PBS (50 mM)/DMSO. Only results for resonances with no overlap with signals of the complexes shown.

128x110mm (400 x 400 DPI)

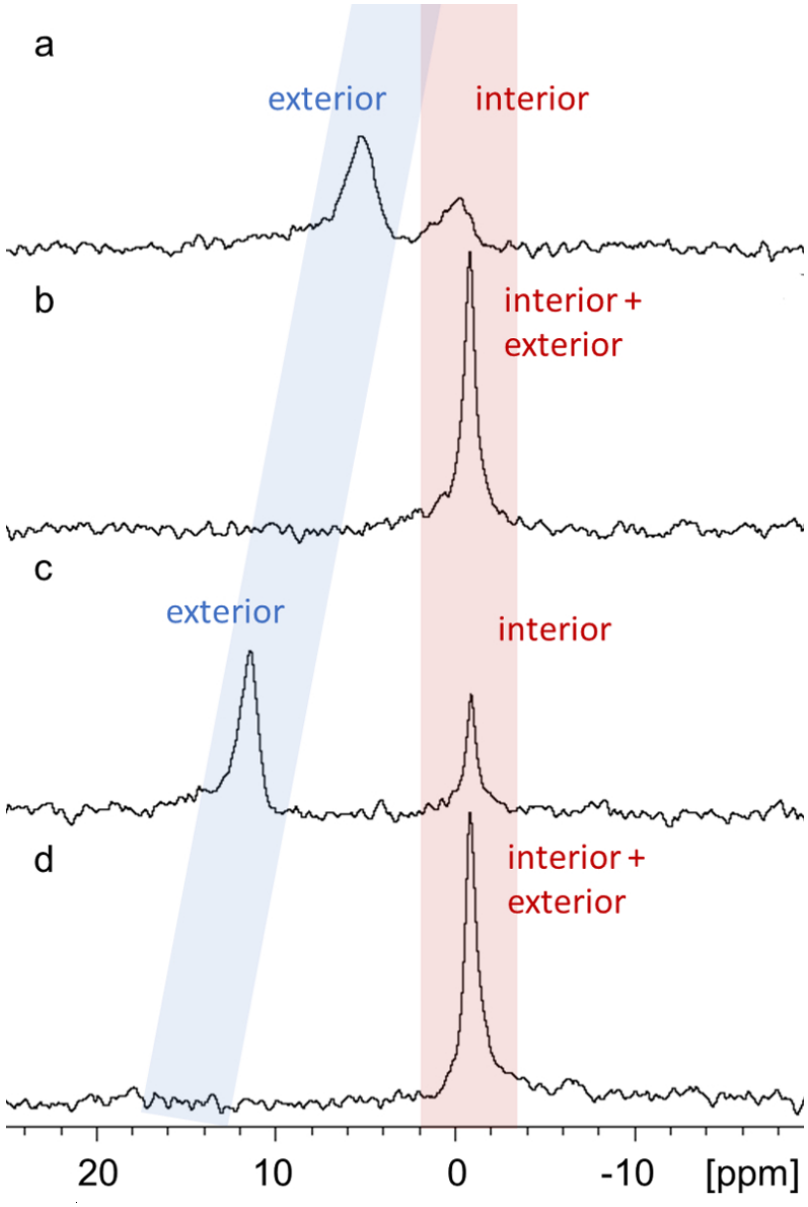

Figure 8. 31P NMR of (a): DOPC (10 mM) vesicles and 1 (1 mM) in presence of 1 mM PrCl3 in D2O/DMSO, (b): DOPC (10 mM) and 1 (1 mM) in D2O/DMSO, (c): DOPC (10 mM) vesicles and PrCl3 (1 mM) in D2O/DMSO, (d): DOPC (10 mM) vesicles in D2O/DMSO.

64x96mm (310 x 310 DPI)

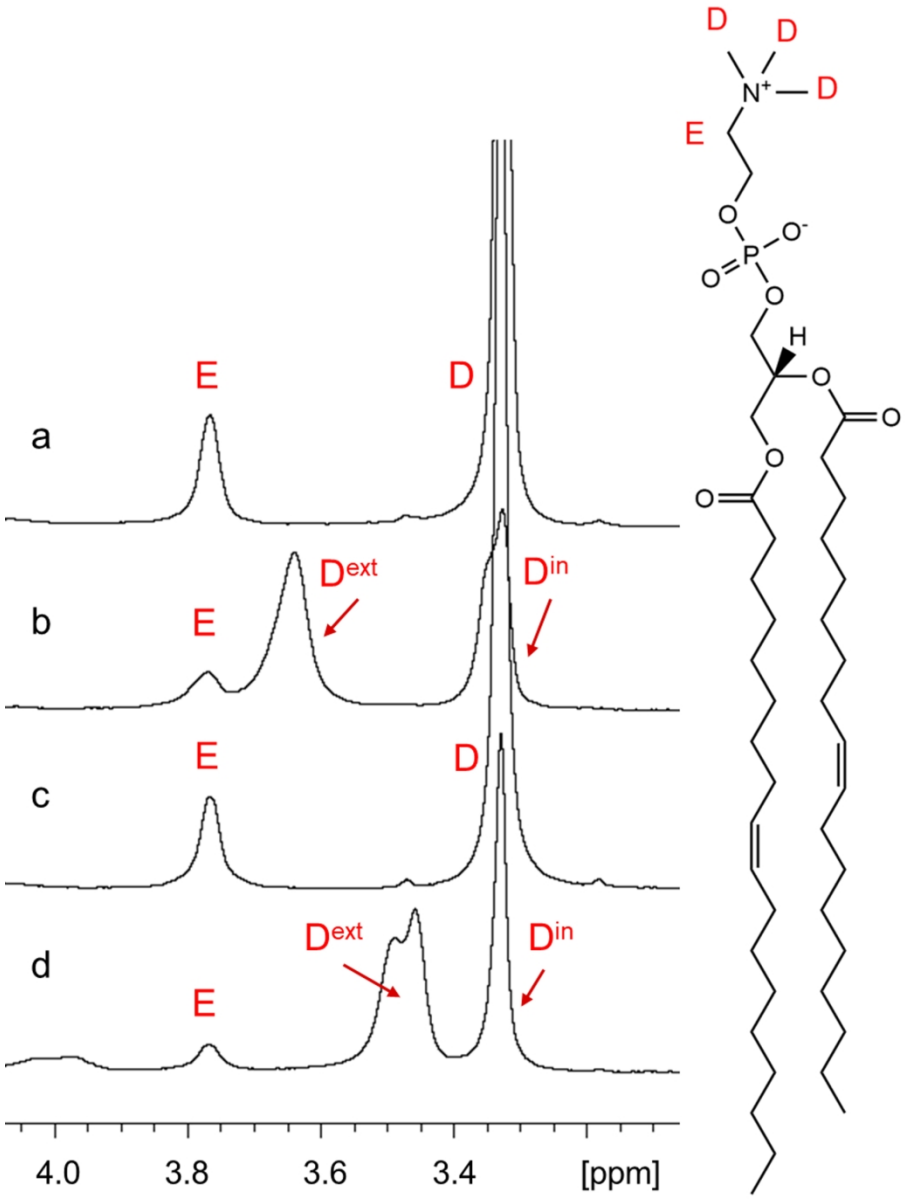

Figure 9. 1H NMR of (a): DOPC (10 mM) vesicles in D2O/DMSO, (b): DOPC (10 mM) vesicles in presence of 1 mM PrCl3 in D2O/DMSO, (c): DOPC (10 mM) vesicles and 1 (1 mM) in D2O/DMSO, (d): DOPC (10 mM) vesicles, 1 (1 mM) and PrCl3 (1 mM) in D2O/DMSO.

77x103mm (600 x 600 DPI)

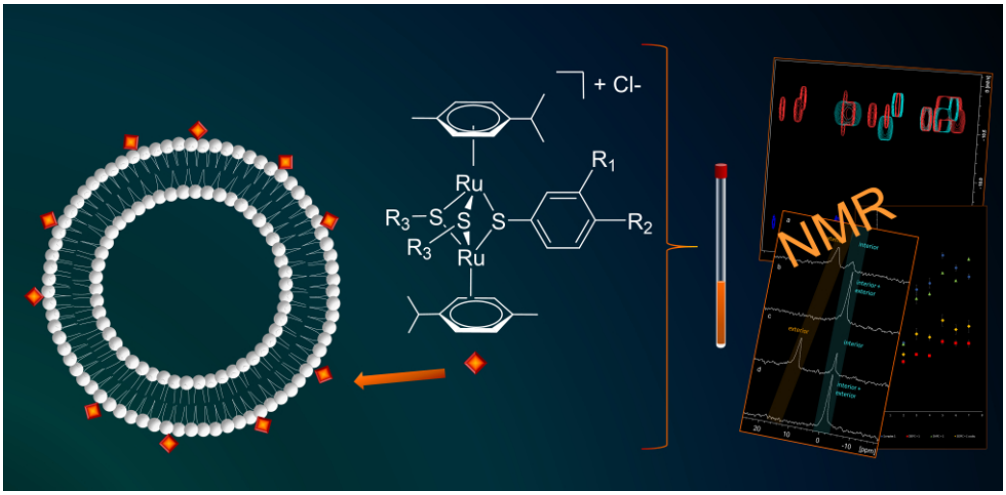

TOC figure

82x40mm (300 x 300 DPI)